Check for updates

Biomass-based graphene aerogel for the removal of emerging pollutants from wastewater

Vijayendra Kumar Tripathi,[a] Manish Shrivastava, [ID][b] Jaya Dwivedi,[a] Raju Kumar Gupta, [ID]*[cdefg] Lokesh Kumar Jangir*[h] and Kumud Malika Tripathi [ID]*[h]

The emerging pollutants present in wastewater have become an important scientific and social concern because of their detrimental effect on human health and the ecosystem. To remove these emerging pollutants from wastewater, the conventional methods are insufficient. Therefore, innovative, cost effective, and efficient approaches are required to handle this rising problem. Biomass-based graphene aerogels showed an effective solution for the removal of emerging pollutants from wastewater because of their exceptional properties, such as large surface area, tunable pore structures, and high adsorption capacity, which make them highly efficient for the removal of a wide range of pollutants. This review article provides a detailed overview of the synthesis techniques of graphene aerogels and highlights the influence of fabrication parameters on the performance of the resulting aerogels. Furthermore, this review discusses emerging pollutants and their classification in detail along with detection of emerging pollutants using graphene aerogels. This review further explores the application potential of biomass-based graphene aerogels in wastewater treatment, such as adsorbents, photocatalysts, graphene aerogel-based membranes, *etc.* emphasizing their capability to remove diverse classes of emerging pollutants. Finally, the conclusion and future prospects in the development and application of biomass-based graphene aerogels for the removal of emerging pollutants from wastewater are discussed. This review underscores the need for further research to optimize the synthesis processes, enhance the adsorption capacity, and evaluate the long-term performance of graphene aerogels in real-world wastewater treatment scenarios.

1. Introduction

The contamination of wastewater with emerging pollutants has become a pressing environmental concern worldwide.[1] Emerging contaminants are a class of chemicals which have recently been identified to have adverse effects on aquatic ecosystems and pose risks to human health.[2] These compounds have diverse chemical nature including endocrine disruptors, pharmaceuticals and personal care products (PPCPs), microplastics, antibiotics, ionic liquids, polycyclic aromatic hydrocarbon derivatives and engineered nanoparticles.[3–5] Emerging pollutants can enter the water through various sources such as industrial activity, agricultural waste, hospitals and household activities, as well as from the improper disposal of pharmaceuticals, expired medicine and other chemicals.[3] Various reports on adverse effects of these emerging pollutants on the ecosystem as well as the methods for their detection and removal have been reported.[6,7] Conventional wastewater treatment processes such as reverse osmosis, flotation, electro-precipitation, membrane separation, flocculation, ion exchange, *etc.* are typically not designed to effectively remove these emerging pollutants, leading to their discharge into water bodies and subsequent environmental consequences.[7,8] Therefore, there is a growing need for advanced and sustainable approaches to address this issue. A wide range of functional materials and technologies have been developed with the aim of purifying contaminated water, thereby ensuring its safety for reuse.[7]

Graphene refers to a solitary layer of carbon having excellent mechanical, thermal and electronic properties.[9]

[a] *Department of Chemistry, Banasthali Vidyapith, Banasthali, Rajasthan-304022, India*

[b] *Department of Chemistry, University of Allahabad, Uttar Pradesh, 211002, India*

[c] *Department of Chemical Engineering, Indian Institute of Technology Kanpur, Kanpur, 208016, UP, India. E-mail: guptark@iitk.ac.in*

[d] *Department of Sustainable Energy Engineering, Indian Institute of Technology Kanpur, Kanpur-208016, UP, India*

[e] *Kotak School of Sustainability, Indian Institute of Technology Kanpur, Kanpur-208016, UP, India*

[f] *Center for Environmental Science and Engineering, Indian Institute of Technology Kanpur, Kanpur-208016, UP, India*

[g] *Chandrakanta Kesavan Centre for Energy Policy and Climate Solutions, Indian Institute of Technology Kanpur, Kanpur-208016, UP, India*

[h] *Department of Chemistry, Indian Institute of Petroleum and Energy, Visakhapatnam, Andhra Pradesh, 530003, India. E-mail: lokesh7785@gmail.com, kumud20010@gmail.com*

This journal is © The Royal Society of Chemistry 2024

React. Chem. Eng., 2024, **9**, 753–776 | 753

Graphene has found extensive utility as an adsorbent and catalyst because of its high effective surface area, tunable band gap and admirable electronic transmission performance.[10] However, its potential is limited by its nano size, agglomeration issues, and difficulty in mass production and maintaining a defect-free structure.[11] The properties of graphene can be further engineered by either composite fabrication or heteroatom doping. Numerous studies have verified that composite fabrication of graphene with a metal–organic framework or other nanomaterials can tune the electrical conductivity of graphene and mitigates the aggregation and restacking tendencies among graphene nanosheets.[12] However, two-dimensional (2D) graphene nanosheets can easily convert back to graphite because of π–π interaction and van der Waals interaction between the graphene nanosheets.[6] The migration of 2D graphene nanosheets to graphite greatly affects their properties. Furthermore, composite fabrication is a tedious process and optimization of the interphase between two constitutes is a great issue. To overcome the aforementioned issues of 2D graphene and related materials, construction of graphene in a three-dimensional (3D) architecture as graphene aerogel is attracting great attention.[13]

Aerogel is a 3D highly porous structure and can be fabricated by substituting the liquid component by gas, typically air. Aerogels of various materials such as carbon fibers,[14] silica[15] and titania[16] have been highly investigated for water remediation and environment applications. Compared with other aerogel materials, graphene aerogel is superior because of its lightweight 3D porous structure consisting of 2D atomic layers which provides maximum specific surface area, lower density, high mechanical strength, chemical stability and greater tunability.[1] Meanwhile, conventional aerogels are fragile and prone to mechanical deformation, and their synthesis methods are more complex and can involve chemicals with environmental concerns. There are various types of graphene aerogels such as graphene oxide aerogel,[17] reduced graphene oxide aerogel,[18] 3D printed graphene aerogel, metal decorated graphene aerogel[19] and natural source derived graphene aerogel.[20] The choice of graphene aerogel depends on the intended application and the specific properties required for that application. Biomass-based graphene aerogels are derived from renewable resources such as plant-based materials and offer a straight-forward synthesis process, cost-effectiveness, and more sustainable and environmentally friendly nature along with excellent adsorption and photocatalytic activity towards contaminants present in water.[20,21] In addition, the characteristics of biomass-derived graphene aerogels can be tuned by selecting specific biomass precursors and optimizing processing conditions that allow for a wide range of applications.[22] Furthermore, to enhance the selectivity and adsorption capacity towards emerging contaminants, biomass-based precursors can introduce heteroatoms and functional groups into the graphene structure. Leão *et al.* highlighted the removal mechanisms for emerging water pollutants, including organic dyes, drugs, heavy metals, pesticides and endocrine disruptors on the basis of the structure and properties of graphene aerogels.[23] Moreover, the methods involving adjustable synthesis and embellishment to regulate the micro, meso, and macro-level structures and active sites are also comprehensively assessed.[13]

The optimization of porosity, surface functionalities and specific surface area is a critical factor to boost up the density of catalytic sites and in consequence adsorption and photocatalysis towards emerging pollutants. For this purpose, several approaches have been adopted, with particular emphasis on enhancing the capabilities towards solvent adsorption,[24] metal removal and adsorption of organic contaminants.[25] For example, the oxygenous functionalities incorporated in graphene aerogel demonstrated significant improvement in adsorption efficiency as compared to graphene aerogel alone. Moreover, the adsorption efficiency was enhanced and more than doubled as compared to commercially available activated carbon.[20] Graphene aerogels and their composites show enhanced photocatalytic activity

Vijayendra Kumar Tripathi received his BSc degree in Chemistry from Christ Church College Kanpur India and MSc degree in Chemistry from DAV College Kanpur India. He is currently a PhD student at the Department of Chemistry, Banasthali Vidyapith, Rajasthan, India. His research work is focused on the synthesis of green nano-carbons for environmental remediation applications.

Vijayendra Kumar Tripathi

Dr. Manish Shrivastava is an Associate Professor at the Department of Chemistry, Central University of Allahabad, Prayagraj, India. He obtained his graduation, post-graduation, and D. Phil (Ph. D.) degree from the Central University of Allahabad, Allahabad. Dr. Srivastava has published over 40 research papers in international journals, along with proceedings, 15 book chapters and two books in international publication. His research interests include nanocatalysts, catalyzed organic synthesis and water pollution.

Manish Shrivastava

754 | *React. Chem. Eng.*, 2024, **9**, 753–776

This journal is © The Royal Society of Chemistry 2024

towards emerging pollutants present in wastewater. The doping of foreign atoms such as boron and nitrogen also enhances the photocatalytic activity towards emerging water pollutants.[13,26] A review report summarized various routes for synthesizing 3D graphene-based materials designed to eliminate emerging pollutants.[23] Furthermore, a comparative study of 2D graphene and 3D graphene-based materials was done for the photocatalytic and adsorption efficiency.[11]

This review aims to provide a comprehensive overview for the synthesis, characteristics, and applications of biomass-based graphene aerogels and their applications in the remediation of emerging pollutants. The utilization of biomass sources as precursors such as agricultural waste, forest residues, and aquatic plants and their suitability for the synthesis of graphene aerogels is compressively reviewed. Special emphasis is focused on the effect of various synthesis

Dr. Jaya Dwivedi is working as a Professor and Head, Department of Chemistry and Dean, School of Life Sciences at Banasthali Vidyapith, Rajasthan, India. Her area of specialization is organic synthesis, material development and natural products. She has published several articles in the journals of national and international repute. Besides, she has also authored a few book chapters with renowned publishing houses.

Jaya Dwivedi

Dr. Raju Kumar Gupta is currently a Professor at the Department of Chemical Engineering, Indian Institute of Technology Kanpur, India. Prof. Gupta obtained his B. Tech in Chemical Engineering from the Indian Institute of Technology Roorkee, India, in 2005 and received his Ph.D. degree in Chemical and Biomolecular Engineering from the National University of Singapore, Singapore in 2010. He joined as an Assistant Professor at

Raju Kumar Gupta

the Department of Chemical Engineering, Indian Institute of Technology Kanpur, India in 2012. Prof. Gupta's research group has made important contributions to the area of sustainable materials, green synthesis, and nanostructured materials for wastewater treatment and energy storage applications. His current research interests are photocatalysis for water remediation and CO_2 capture & conversion to fuels, water generation via desalination and fog harvesting, perovskite solar cells and energy storage devices based on batteries. Prof. Gupta has been the recipient of several fellowships and awards for his outstanding career in academic and research fields. Some of the fellowships and awards include DST Inspire Faculty Award 2013, IEI Young Engineer Award (2014–15), Young Scientist Award (2014–15), P. K. Kelkar Young Faculty Research Fellowship 2018, Distinguished Young Alumnus Awards 2021, PK Kelkar Young Faculty Fellowship 2022 and Fellowship of the Royal Society of Chemistry (FRSC) 2022. He has authored more than 130 research articles in international journals, 6 patents, 3 edited books, and 18 book chapters and guest edited special issues for several international journals, and his work has been cited more than 10 000 times. Prof. Gupta is an editorial board member of several international journals, as well as a member of scientific bodies. Some of his significant appointments include Editor for Elsevier journal 'Sustainable Chemistry One World', Associate Editor for Elsevier journal 'Solar Energy', Editorial Board member for Nature Research journal 'Scientific Reports', Wiley journals 'IET Nanodielectrics' & 'Journal of Polymer Science', and Elsevier journal 'Current Opinion in Green and Sustainable Chemistry', and Editorial Advisory Board member for ACS journal 'Environmental Science & Technology Water' and Royal Society of Chemistry journals 'Nanoscale Horizons', 'Reaction Chemistry & Engineering' and 'Molecular Systems Design & Engineering'.

This journal is © The Royal Society of Chemistry 2024

React. Chem. Eng., 2024, **9**, 753–776 | 755

parameters, such as carbonization temperature, activation methods, and doping approaches, on the performance of graphene aerogels. Furthermore, the mechanisms of different techniques for water remediation especially adsorption and photodegradation along with the factors affecting their efficiency are critically evaluated. This review will also highlight the application potential of biomass-based graphene aerogels in wastewater treatment, focusing on their ability to remove a wide range of emerging pollutants. The scalability, reusability, and regeneration of graphene aerogels will be discussed to assess their economic feasibility and environmental sustainability. Challenges and future prospects in the development and application of biomass-based graphene aerogels for wastewater treatment will also be addressed. The findings presented in this review can help as a valuable resource for researchers, scientists, and industries involved in the field of wastewater treatment and environmental remediation. The schematic of the overview of the review is shown in Scheme 1.

2. Recent trends in biomass-based graphene aerogels

Currently, graphene aerogels are attracting enormous attention in every aspect of water remediation technologies because of their novel structural characteristics. The utilization of renewable biomass-derived graphene aerogels reduces the reliance on fossil-derived resources and sustainable materials. A 3D architecture of graphene aerogel with an ultra-low density, excellent swilling ability and strong

mechanical stability can be achieved by a one-pot green fabrication method using high energy γ-ray irradiation for the removal of hazardous pollutants from wastewater.[27] The assembly of a dual-functional graphene aerogel guided by bayberry tannin was utilized for the simultaneous solar steam generation and extraction of uranium (230.10 mg g^{-1}) from sea water. In the synthesis process, bayberry tannin was uniformly decorated inside the pores of graphene aerogels, integrating the binding between bayberry tannin and uranium.[28] The selective uranium capture (654.2 mg g^{-1}) was enhanced by the appropriate functionalization of β-cyclodextrin/graphene aerogel using amidoxime.[29] The functionalization of the graphene aerogel provided sufficient confinement and relatively high surface area which enhanced its adsorption capacity. Pang et al. demonstrated the hydro plastic foaming (HPF) technique for the direct conversion of graphene oxide (GO) into graphene aerogel with continuous large area micro arrays. The synthesis mechanism of graphene aerogel involved water plasticization, bubble foaming, and direct drying as demonstrated in Fig. 1a. The penetration of water molecules in the interlayer gallery of GO takes place as its solid films come into contact with water and the hydrophilicity driven interaction is completed in a few seconds (Fig. 1b). The activated mobility of GO sheets enables them to reposition themselves by sheet slippage and deformation to adapt the bubble growth (Fig. 1c). Finally, the cluster of bubbles and the adaptable graphene oxide walls bind together to form graphene aerogel by the capillary force during drying (Fig. 1d). The scanning electron microscopy (SEM) image of the prepared graphene aerogel is shown in
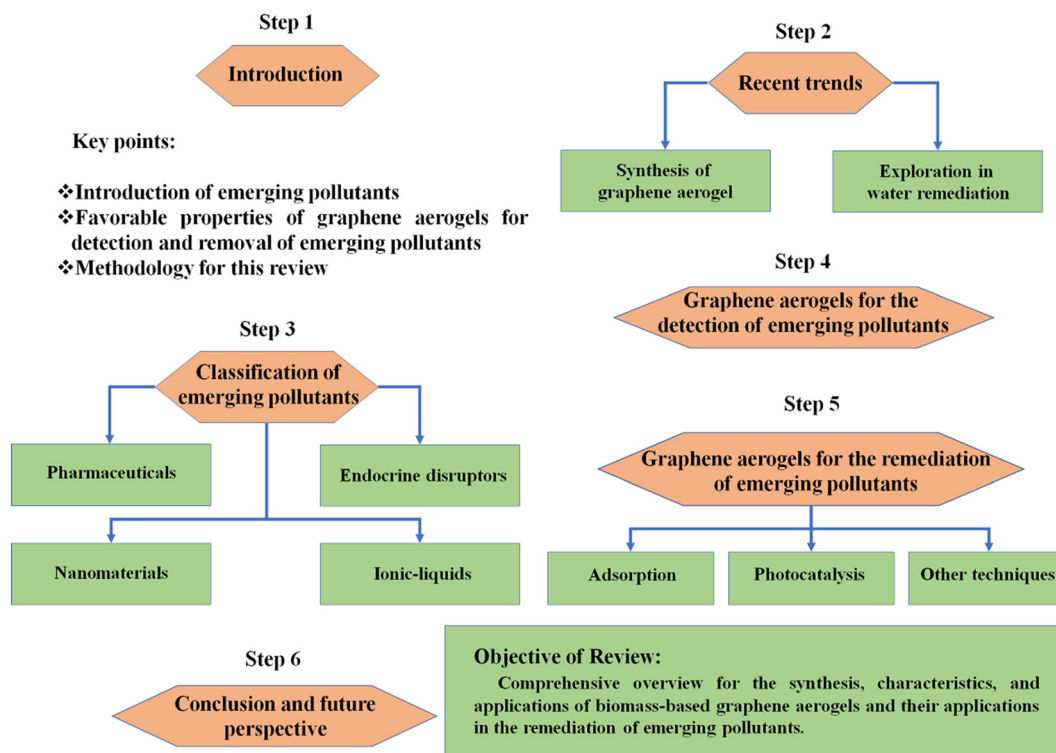
Dr. Lokesh Kumar Jangir earned his PhD in Physics from MNIT Jaipur (2018), M.Tech. degree in Computer Science and Data Processing from IIT Kharagpur (2012), M.Sc. in Physics from the University of Rajasthan (2009), and B.Sc. from the University of Rajasthan (2006). He is currently working as a post-doctoral fellow at IIT BHU Varanasi. His research interests are nanomaterials for optoelectronics, block copolymer nanotemplates, and carbon nanostructures for energy applications.

Lokesh Kumar Jangir

Dr. Kumud Malika Tripathi is a Ramalingaswami faculty/ Assistant Professor at the Department of Chemistry, Indian Institute of Petroleum and Energy, Visakhapatnam, India. She earned her PhD in Chemistry from the Indian Institute of Technology, Kanpur, in 2013. Before joining IIPE, she held several positions, including Assistant Professor at Gachon University, South Korea and postdoctoral fellow at the University of South Brittany, Lorient, France and IIT Kanpur, India. Her research activities include the green synthesis of multifunctional nanomaterials for energy, healthcare and environmental applications. Kumud works at the interface of chemistry, materials science and biology, exploring new nanomaterial-based strategies for environmental monitoring and remediation, self-recharge power units, energy storage devices, CO$_2$ capture and conversion, flexible electronics and photocatalytic water splitting for green hydrogen production.

Kumud Malika Tripathi

Scheme 1 Schematic representation of the review.

Fig. 1e and the three-bubble contact model is illustrated in the inset of Fig. 1e.[30]

Pioneering work from Sharma *et al.* showed a scalable approach for water remediation using GO-based silica aerogel. The doping of GO in silica aerogel was done in a customized high vacuum using a supercritical method.[3] The emerging contaminant removal studies were performed in 100 mL of solution, as demonstrated in Fig. 2a. The removal efficiency underwent additional testing in a semi-batch scale study, as illustrated in Fig. 2b, where a controlled flow rate was maintained through a packed column of aerogel. Additionally, a continuous process for the elimination of emerging contaminants, and a readily scalable approach by utilizing an aerogel-packed reactor was examined using the experimental setup as depicted in Fig. 2c. The maximum removal efficiency of harmful dyes acid green 25 (AG) and crystal violet (CV) was found to be 98.23% and 98.71%, respectively, whereas for sulfamethoxazole (SMA) it was 94.46% as shown in Fig. 2d.[3] Shukla *et al.* reported efficient adsorptive removal of histamine from red wine using a crude biomass derived graphene aerogel. The designed setup could contain a contaminated liquid sample and the flow rate of liquid can be regulated by N_2 pressure.[31] A graphene/biomass aerogel based pressure sensor was fabricated by Wei and coworkers using bacterial cellulose (BC) and caffeic acid. Fig. 2e illustrates the synthesis process of reduced graphene oxide (rGO)@BC and the sensing platform, and Fig. 2f shows the regular and more obvious response to strain.[32]

A cellular structured graphene aerogel for electromagnetic wave absorption was also reported as shown in Fig. 3. The higher porosity of the graphene aerogel results in conductive losses, whereas lower porosity results in polarization losses because of impedance mismatching. The intermediate pore structure provides a cellular structure which leads to multiple scattering of electromagnetic waves in the graphene aerogel and enhances the absorption capacity.[33] Cao *et al.* reported the structural optimization of a graphene aerogel-based composite with many loading sites for metal/non-metal atoms, metal compounds, non-metal compounds and bimetal compounds to enhance adsorption capacities, redox capacities and electrical conductivities.[34] Zhang *et al.* performed infiltration of a monolithic polyimine vitrimer into the pores of graphene aerogels followed by thermal treatment for synthesis of cylindrical monolithic polyimine vitrimer/graphene composites. The prepared composites showed durable compressibility, high compressive strength, high elasticity, high conductivity, and excellent piezoresistive properties.[35]

The tailored pore structure and surface functionalization of biomass-based graphene aerogels are also key parameters to introduce specific functional groups for the further enhancement of the adsorption sites and improve the selectivity of graphene aerogels towards emerging pollutant removal. For example, Lee *et al.* demonstrated the functionalization of graphene aerogels with phenothiazine to enhance the electrochemical active surface area and diffusion behavior by a one-step approach.[36] The polylysine

This journal is © The Royal Society of Chemistry 2024
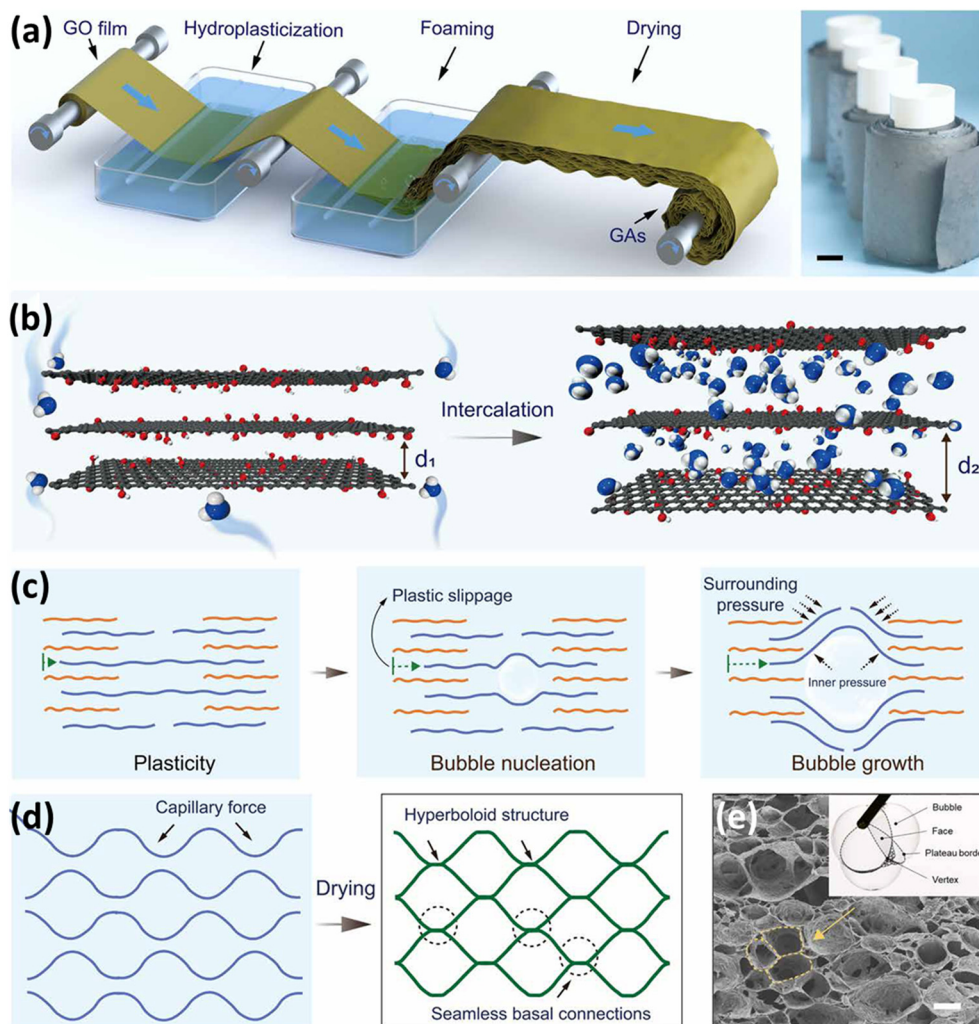
React. Chem. Eng., 2024, **9**, 753–776 | 757

Fig. 1 Synthesis and mechanism of graphene aerogel. (a) The process of HPF. The graphene oxide solid film was continuously transformed into rolled graphene aerogels. (b) The intercalation of water into the graphene oxide solid to expand the interlayer spacing. (c) Self-structural adjustment of graphene oxide layers through plastic slippage to conform to the bubbling process to maintain structural integrity and avoid catastrophic expanding burst. (d) Seamless basal connections of graphene sheets formed by capillary-driven bubble clustering after drying. (e) SEM images of dried graphene aerogel and the corresponding structural model of three-bubble connection (inset). Scale bars, 3 cm (a) and 200 mm (e). Reproduced from ref. 30 with permission from [*Science Advances*], copyright [2020].

functionalization was found to enhance the adsorption capacity of graphene aerogel towards the contaminants present in wastewater.[37] Overall, recent trends are driving advancements in the field and expanding the ability of biomass-derived graphene aerogels for various environmental and technological applications.

2.1 Synthesis of graphene aerogels

Graphene aerogels are 3D porous structures containing a multilayer of carbon atoms which makes the synthesis process more difficult. In order to achieve the requirement of different applications, various techniques have been adopted for the synthesis of graphene aerogels. Herein, we summarized efficient and most commonly used methods for the synthesis of diverse graphene aerogels.

Hydrothermal reduction is the most widely used method for the synthesis of graphene aerogels using GO as a precursor. The process involves 3D graphene hydrogel formation by the addition of metal ions[38] or a polymer[39] as a crosslinking agent in GO dispersion followed by removal of water from the hydrogel while maintaining the pore structure, through electrochemical deposition or centrifugation or the direct freeze-drying method. Ma *et al.* demonstrated the formation of graphene aerogels from Enteromorpha, DI water and GO. They synthesized a graphene aerogel, an ethylene graphene aerogel, and a polyethylene graphene aerogel just by varying polyethylene glycol molecular weights, polyethylene glycol doses, and the ratio of Enteromorpha and GO as shown in Fig. 4a.[39] It was also observed that the adsorption sites of graphene aerogels can be enhanced by the synthesis of a nitrogen-functionalized graphene aerogel with a stereoscopic structure.[26] The macropores and specific surface area of

758 | *React. Chem. Eng.*, 2024, **9**, 753–776
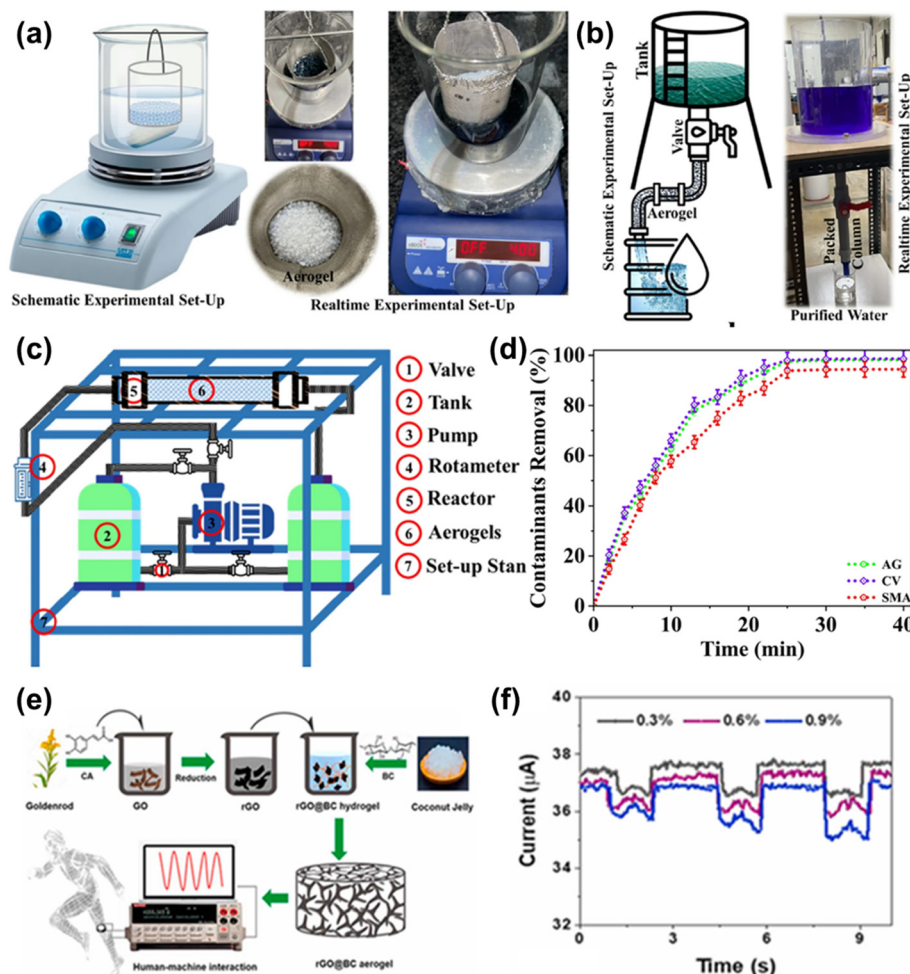
This journal is © The Royal Society of Chemistry 2024

Fig. 2 Experimental setup: (a) batch experiments, (b) semi-batch experiments with an aerogel packed column and controlled flow due to gravity and (c) continuous reactor packed with aerogels. (d) Removal efficiency. Reproduced from ref. 3 with permission from [*Scientific Reports*], copyright [2023]. (e) Schematic illustration of the overall preparation procedure of the rGO@BC aerogel and sensing platform and (f) the limit of detection of the sensor response to strain. Reproduced from ref. 32 with permission from [Elsevier Ltd.], copyright [2021].

graphene aerogels can also be enhanced *via* the formation of 3D networks of self-assembled graphene hydrogel interconnected with metal nanoparticles (NPs). One such example is introduction of copper (Cu) NPs.[40] Oxidized metal ions such as Fe_3O_4 and Fe_2O_3 were also explored for the generation of 3D network structures, which supports the rationality of using oxidized metal ions as crosslinking agents.[38] Besides metal ions, various polymers were also explored as cross-linking agents for the fabrication of highly porous 3D graphene aerogels.[39] Myung *et al.* demonstrated the utilization of pear fruit for the synthesis of a graphene aerogel *via* the combination of hydrothermal and pyrolysis approaches as demonstrated in Fig. 4b.[41] The hydrothermal carbonization of biomass involves various reactions, including dehydration, aromatization, and carbonization, achieved by intermolecular dehydration steps.[41] Although synthesized graphene aerogels *via* the hydrothermal process showed various merits in various applications such as water purification and energy storage, the main drawbacks lie in the synthesis process, which involves a multi-step process, a requirement of chemical activation to enhance the specific surface area, formation of harmful by-products, and acidic waste. To overcome these obstacles, the same group further reported a unique process for the synthesis of 3D graphene aerogels, which involves one-step carbonization of glucose and ammonium chloride without requiring a catalyst, as illustrated in Fig. 4c.[42] Ammonia was bubbled in glucose and formed a 3D structure in an argon environment. The ammonia was generated by the breakdown of ammonium chloride under heat treatment. Incorporation of ammonia into glucose led to the formation of an interconnected porous 3D network as it polymerized at elevated temperatures. Following this, the mixture underwent carbonization at 1100 °C and graphitization was achieved.[42]

Compared to hydrothermal reduction, chemical reduction of GO is a fast process and is executed under a low temperature environment (50–100 °C) for the synthesis of graphene aerogels from GO. A 3D network can be formed by the π–π interactions induced upon reduction of GO. The mostly used reducing agents are ʟ-ascorbic acid, $NaBH_4$, hydrazine, and hydrogen iodide (HI).[43,44] The π–π interactions between rGO sheets are

This journal is © The Royal Society of Chemistry 2024

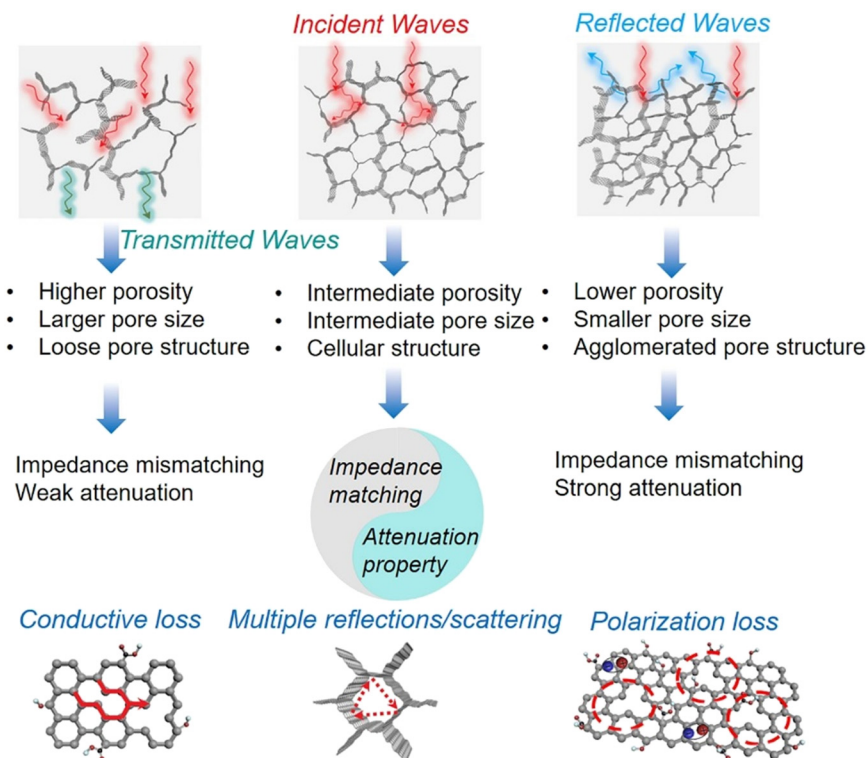*React. Chem. Eng.*, 2024, **9**, 753–776 | **759**

Fig. 3 Schematic illustration of the electromagnetic wave absorption mechanism of graphene aerogels. Reproduced from ref. 33 with permission from [Elsevier B.V.], copyright [2021].

enhanced under slow reduction and lead to the formation of 3D graphene aerogels. The physicochemical properties of graphene aerogels can be controlled by the variation of synthesis parameters such as temperature, reaction time, and content of the precursor and reducing agent.[45] A graphene aerogel was synthesized by mixing of different amounts of ethylene diamine in GO followed by the freeze drying method. The variation in density and pore size was found to be ethylene diamine content dependent.[46] The synthesis method for a superhydrophobic neat graphene aerogel was shown by Xu *et al.* using an *in situ* chemical reduction technique. The prepared aerogel exhibited ultra-low density, a superhydrophobic surface and cross section, and excellent absorption capacity of oil and organic solvents.[47] In order to lower the synthesis expenses, Liang *et al.* reported a green strategy for the synthesis of a scalable 3D macroscopic graphene aerogel using polyethylenimine (PEI) both as a reducing agent and as a crosslinking agent.[48]

Shadkam *et al.* fabricated a graphene aerogel *via* chemical reduction of GO by taking L-ascorbic acid (L-AA) and sodium bisulfite (NaHSO$_3$) as the reduction media, which convert GO into its reduced form, resulting in the formation of the graphene aerogel (GASL).[43] The dissociation of NaHSO$_3$ in aqueous media produces HSO$_3^-$ which attacks the C–O bond and replaces it with the C–S bond. Subsequently, the available free oxygen was protonated immediately leading to the discharge of a water molecule. Finally, SO$_3$ molecules were separated from rGO sheets and transformed into soluble SO$_4^{2-}$ ions which can be effortlessly washed out from the system.

Furthermore, the cross-linkage caused by LAA's by-products provides structural stability to the final product as depicted in Fig. 4d.[43] Dehydroascorbic acid converted into oxalic and guluronic acid by the deprotonation of L-AA molecules. The strong hydrogen bond formation between these species and residual oxygen on rGO sheets prevents rGO sheets from restacking through π–π interactions.[43] Wang *et al.* proposed a one-step chemical reduction method for the fabrication of a graphene aerogel which is composed of rGO, Al and Bi$_2$O$_3$ NPs. The introduction of ethylenediamine in the dispersed solution of rGO, Al and Bi$_2$O$_3$ starts the reaction for gel formation without affecting the chemical reactivity of Al and Bi$_2$O$_3$. The reaction mechanism is illustrated in Fig. 4e.[49] Although chemical reduction is a fast process, it has certain limitations such as lack of selectivity and control, unwanted side reactions, reaction conductions (maintaining temperature and pH), and environmental impact due to the formation of unintended by-products.

Template guidance is an effective method to construct a 3D porous graphene network with any specific shape and structure of the layered membrane.[50] This is an effective method for the synthesis of a 3D structure of any specific shape.[51] The pore size and pore distribution of the synthesized graphene aerogels in this method can be controlled by using different templates, and the specific surface area can be controlled by varying the concentration of the source.[50,52] An ultrathin carbon aerogel was synthesized using cubic NaCl crystals as a template. A gelatin hydrogel was filled in the confined space between the
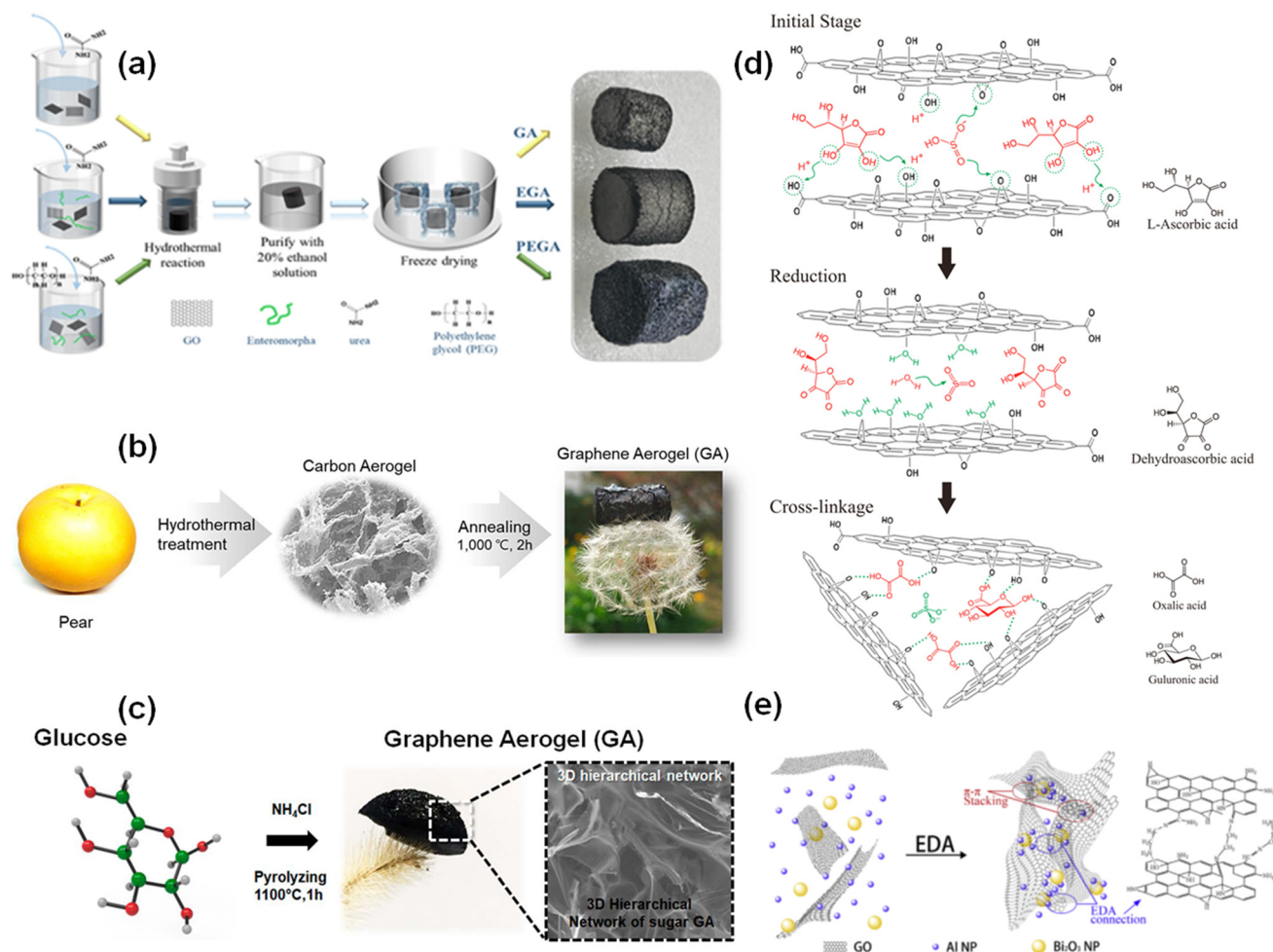
760 | *React. Chem. Eng.*, 2024, **9**, 753–776

This journal is © The Royal Society of Chemistry 2024

Fig. 4 (a) Synthesis scheme of three kinds of aerogels; reproduced from ref. 39 with permission from [Elsevier Inc.], copyright [2022]. (b) Schematic of a biomass derived graphene aerogel; reproduced from ref. 41 with permission from [American Chemical Society], copyright [2019]. (c) Schematic representation for the synthesis of a graphene aerogel from a sugar source; reproduced from ref. 42 with permission from [American Chemical Society], copyright [2019]. (d) Schematic illustration of the reduction reaction and cross-linking in the formation of a graphene aerogel; reproduced from ref. 43 with permission from [Elsevier Ltd], copyright [2020]. (e) Synthesis mechanism of an rGO/Al/Bi$_2$O$_3$ aerogel; reproduced from ref. 49 with permission from [The Combustion Institute. Published by Elsevier Inc.], copyright [2018].

NaCl crystals followed by thermal annealing at high temperature. The formation of ultrathin carbon aerogels takes place after removal of the NaCl templates with water.[53] Chen *et al.* demonstrated the template assisted chemical vapor deposition (CVD) method for the synthesis of a graphene aerogel.[51] A high temperature CVD method was used by Yu *et al.* for the fabrication of ultra-light graphene-amorphous hierarchical foam in which Cu foam was used as a sacrificial template, providing well defined structures, and amorphous carbon was used with improved durability and mechanical flexibility of the structure.[54] However, multiple steps, the use of hazardous reagents for removal of the template, and required high annealing temperatures are barriers to process scalability.

The morphological investigation of graphene aerogels is usually done by SEM. The low magnification SEM image in Fig. 5a shows the 3D microporous interconnected structure of a graphene aerogel with high surface area and porosity. Fig. 5b presents the high magnification image showing randomly oriented interconnected graphene sheets. The high-resolution SEM (HR-SEM) image in Fig. 5c shows crumpled and folded orientations of graphene sheets. The transmission electron microscopy (TEM) image shown in Fig. 5d confirms the existence of wrinkled graphene nanosheets in the sample. The white circle in Fig. 5e shows missing graphitic planes in the aerogels. The high-resolution TEM (HR-TEM) image of graphene aerogels shown in Fig. 5f confirms the presence of lattice fringes and surface defects as indicated by white arrows. The X-ray diffraction (XRD) spectrum demonstrated in Fig. 5g indicates the semi-crystalline nature of graphene aerogels. The (002) and (100) planes at peak positions $2\theta = 25.02°$ and $43.81°$, respectively, confirm the occurrence of interlayer condensation and identification of a turbostratic carbon structure.[42] The nitrogen sorption measurements (Fig. 5h) of graphene aerogels synthesized from pear shows a high Brunauer–Emmett–Teller (BET) surface area of around 1001 m^2 g^{-1} with a pore volume of 0.68 cm^3 g^{-1}. Fig. 5i shows the pore size distribution profile of aerogels computed using nonlocal density functional theory.[41]

This journal is © The Royal Society of Chemistry 2024

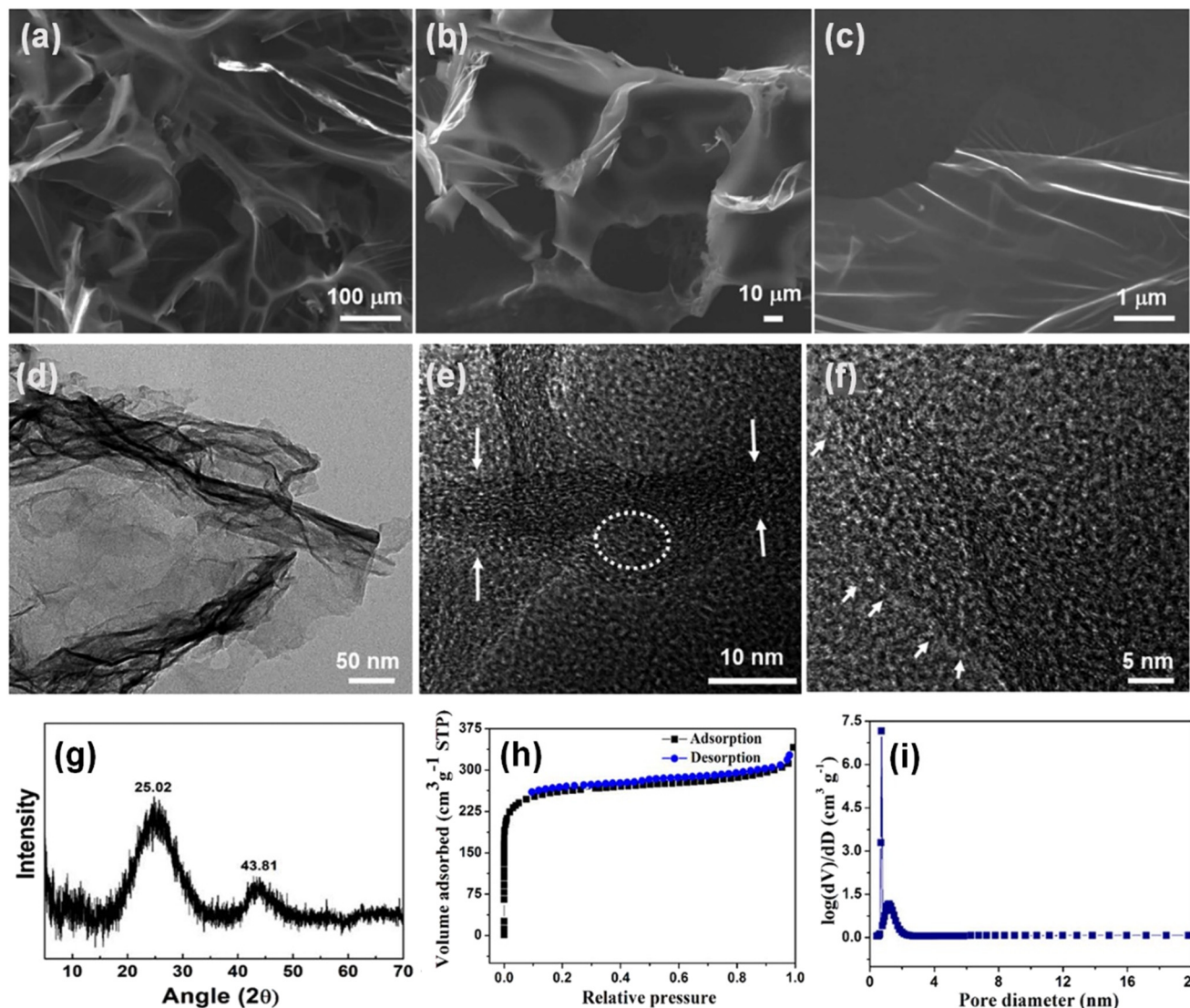*React. Chem. Eng.*, 2024, **9**, 753–776 | **761**

Fig. 5 Morphological and structural characterization of the graphene aerogel; (a) low-magnification SEM image; (b) high-resolution SEM image; (c) high-resolution SEM image showing a sheet like morphology; (d) TEM image of the graphene aerogel; (e) HR-TEM image showing surface defects marked by white arrows and a circle; (f) HR-TEM image showing the crystal lattice defects; (g) XRD spectrum of the graphene aerogel. Reproduced from ref. 42 with permission from [American Chemical Society], copyright [2019]. (h) Nitrogen adsorption/desorption isotherms of graphene aerogels and (i) pore size distribution curve of graphene aerogels. Reproduced from ref. 41 with permission from [American Chemical Society], copyright [2019].

The synthesis methods discussed above are most commonly used for the synthesis of graphene aerogels. However, a modification and specific variation can be done depending on the desired properties and applications.

2.2 Exploration of graphene aerogels in water remediation

Graphene aerogels have unique properties which make them promising materials for water remediation.[55] In this subsection, we focused on the potential of graphene aerogels for the removal of various emerging contaminants. High surface area and the presence of functional groups on the surface of graphene aerogels enable strong adsorption interactions with emerging water contaminants.[4] Graphene aerogels demonstrated admirable adsorption capacity towards the emerging pollutants because of π–π stacking interactions, hydrogen bonding, and electrostatic interactions.[56] The surface functionalization and composite formation enhance the adsorption capacity and selectivity to specific pollutants.[4,57] For example, loading of copper NPs and doping of F in graphene aerogel enhance the adsorption of perfluorooctanoic acid by 2.68 times.[57] Han *et al.* demonstrated the potential of a graphene–boron nitride composite aerogel for the adsorptive removal of pharmaceutical ciprofloxacin from wastewater. The composite foam showed an excellent removal efficiency of ~99%.[58] In another study, a graphene-based aerogel was synthesized using GO sheets by an ice segregation induced self-assembly method. The prepared sample showed superior

adsorption capacities towards emerging pollutants such as phenol and bisphenol.[59] Fruit waste derived cellulose was used for the gelatinization of graphene oxide to produce a highly porous and ultra-light composite aerogel for organic pollutant adsorption from wastewater. The interconnection between GO sheets and the cellulosic skeleton generated macroscopic porosity *via* a hydrogen bonding network helpful for the transport and diffusion of organic contaminants. Consequently, the adsorption process was governed by the active surface sites of the aerogel composite and the charge, size, and chemical structure of emerging pollutants.[60] A lignin biomass modified graphene aerogel showed superior adsorption capacity than the graphene aerogel for the adsorption of petroleum oils along with toxic solvents like chloroform, carbon tetrachloride, and toluene. Furthermore, the adsorption capacity can be improved by thermal treatment of the prepared sample.[61] In addition to adsorption, graphene aerogels can also be utilized as catalysts for the degradation of emerging pollutants in water. The high surface area and porous structure of graphene aerogels enable the activation of peroxides or persulfates, for advanced oxidation processes.[62] The degradation of organic pollutants into harmless by-products takes place because of the catalytic properties of graphene aerogels.[62] A WS_2 nanosheet incorporated N-doped rGO aerogel showed photodegradation of caffeine up to 93% within 180 min in different real matrices.[55] The N-doped graphene aerogel demonstrated catalytic degradation of antibiotics from wastewater. The as-synthesized sample showed superior catalytic activity towards ibuprofen because of the synergistic effects of the porous structure and N-doping in the sp^2-hybridized aerogel.[63] A microwave assisted degradation technique was also utilized for the removal of emerging contaminants. An nZVI incorporated N-rGO aerogel eliminated almost 100% imidacloprid within 2 min in a solution of 10 mg L^{-1} under microwave irradiation.[64] Incorporation of graphene aerogels into a membrane system offers enhancement in water purification processes. The porous structure of graphene aerogels enables the efficient filtration and separation of contaminants, whereas their chemical stability favors the long-term performance.[65] Moreover, graphene aerogels exhibit inherent antimicrobial activity which prevents biofilm formation and growth of bacteria, making them suitable for the removal of bacteria and microbial contaminants from water sources.[19,66] Graphene aerogels are continuously explored in water remediation as they are promising materials for addressing the challenges associated with water pollution and ensuring access to clean and safe water resources.

3. Emerging pollutants and their detection using graphene aerogels

Emerging pollutants are those chemical substances which adversely affect the environment and human health but are not yet widely regulated. The primary sources of emerging pollutants are industrial and agricultural waste, PPCPs, endocrine disruptors (EDCs), engineered NPs, pesticide metabolites and transformation products.[67]

PPCPs are the class of emerging pollutants which includes drugs, antibiotics,[68] hormones, fragrances, cosmetics, and sunscreen agents.[69] PPCPs enter the environment through various natural and anthropogenic activities.[67] PPCPs do not readily degrade and can travel through different environmental compartments. Some PPCPs at low concentrations can disrupt the endocrine and reproduction systems, which results in behavioral changes.[70] The presence of antibiotics in the ecosystem enhances the antibiotic resistance in bacteria, which reduces their effectiveness in the medical treatment.[71] Low concentrations of PPCPs have been detected in drinking water sources which with long-term exposure can give rise to health issues.[2] It is necessary to develop strategies for the monitoring, assessment, and regulation of PPCPs, which include proper medication disposal and improved water treatment technology. Graphene aerogels hold significant potential for the detection and removal of emerging pollutants due to their high surface area, porous structure, excellent conductivity, and chemical stability.[72] The easy regeneration and reuse make them cost-effective and environmentally friendly for repeated pollutant detection and elimination.[73] The functionalization of graphene aerogels improved their sensing performance towards PPCPs. A functionalized rGO aerogel was adopted for the electrochemical sensing of catechol. The large surface area and the presence of catalytically active sites on the surface of the aerogel/carbon plate electrode enable remarkable selectivity and sensitivity for catechol.[17] A sensor based on the composite of VS_2 quantum dots, a 3D N,S-doped graphene aerogel and CNTs (VS_2-QDs/GNA/cCNTs) was proposed for electrochemical sensing of azithromycin (AZM) and hydroxychloroquine (HCQ). The excellent performance of the prepared sensor was due to the synergistic effects of the composite, the high electron transfer rate, and the large number of catalytically active sites on the surface of the electrode.[74] Fig. 6a illustrates that upon increasing the cyclic voltammetry scan rate of potential from 30 mV s^{-1} to 300 mV s^{-1}, the peak current increased with a shift in oxidation potential to a more positive value for both AZM and HCQ. In addition, the oxidation of AZM and HCQ in the buffer solution of B.R. at pH 6 is demonstrated in Fig. 6b.[74]

EDCs are another class of emerging pollutants that disturb the immune system of humans and wildlife even in a trace amount.[76] EDCs include bisphenol A (BPA), dioxin, phthalates, and certain pesticides which can be neurotoxic,[77] reproductive toxic,[78] genotoxic and carcinogenic.[79] The main sources of entering EDCs in the environment include wastewater discharge, improper disposal practices, and agricultural runoff.[80] The synthesis, secretion, transport, and binding of hormones can be blocked, mimicked, or altered by EDCs, which can also affect other aspects of the endocrine system.[81] They can disrupt hormone signaling pathways, bind to hormone receptors, or alter hormone metabolism, causing problems in physiology and development.[82] Moreover, EDCs can pose risks during critical developmental stages and early childhood by affecting the natural hormonal mediated processes.[83] Exposure
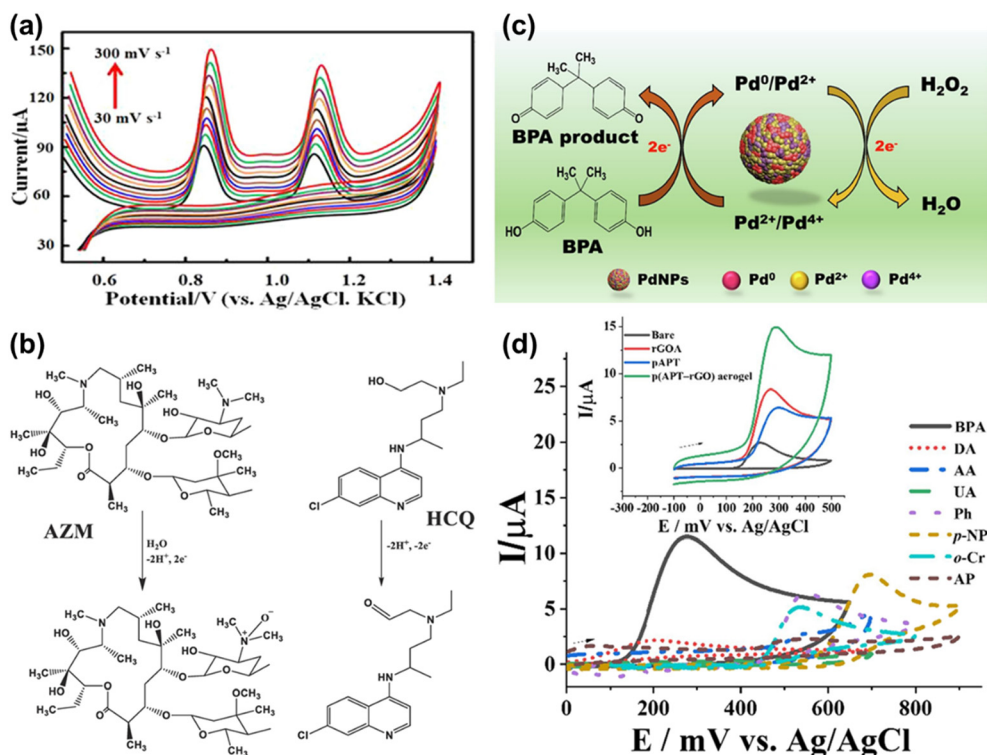
Fig. 6 (a) CV scans of 15.0 μM AZM and HCQ at VS$_2$ QDs/3D N,S@ GNA/cCNTs/GCE in B.R. buffer (pH 6.0) at a scan rate of 200 mV s^{-1} after a preconcentration time of 150 s. (b) The electrochemical oxidation of AZM and HCQ at VS$_2$ QDs/3D N,S@GNA/cCNTs/GCE in B.R. buffer (pH 6.0). Reproduced from ref. 74 with permission from [Elsevier B.V.], copyright [2021]. (c) The proposed mechanism of the Pd NPs on the RGA–PEI–Pd composite electrode in BPA oxidation and H$_2$O$_2$ reduction. Reproduced from ref. 18 with permission from [Elsevier B.V.], copyright [2021]. (d) CVs obtained at the *p*(APT–rGO) aerogel electrode in 0.1 M PBS (pH 7.0) containing 50 μM DA, AA, UA, Ph, *p*-NP *o*-Cr, and AP, and 20 μM BPA (the inset show CVs in response to 20 μM BPA for different modified electrodes). Reproduced from ref. 75 with permission from [Elsevier B.V.], copyright [2022].

to EDCs in aquatic environments also impacts wildlife populations by disturbing reproductive success and sexual development.[84] BPA has been found to be the highest volume of chemical produced worldwide. BPA has been detected in plastic bottles and food storage cans with epoxy resins and also detected in environmental samples, such as dust, air, and water.[85] High concentrations of BPA were found in surface water, tap water, landfill leachate and Antarctic glacier.[86,87] Dioxins are another class of EDCs in the environment because of natural processes such as forest fires and volcano emission which have only a small proportion of these chemical contaminants.[88] Furthermore, melting of metals, combustion of coal and petroleum, PVC plastic production, chlorinated pesticide production, and white paper pulp treatment with chlorine are the industrial sources of dioxin in the environment.[89,90] The detection of endocrine-disrupting properties of chemicals requires comprehensive testing approaches and their regulation is challenging.[91] A Pd NP embedded PEI–rGO aerogel was utilized for the electrochemical detection of BPA and H$_2$O$_2$. In the detection process, Pd contributes to oxidation of BPA and reduction of H$_2$O$_2$ as demonstrated in Fig. 6c.[18] In another report, a similar endocrine disruptor was electrochemically detected by an rGO–polyterthiophene composite (*p*(APT–rGO)) aerogel based sensor

with an improved detection limit.[75] Fig. 6d shows the CV responses for BPA, dopamine (DA), ascorbic acid (AA), uric acid (UA), phenol (Ph), *p*-nitrophenol (*p*-NP), *o*-cresol (*o*-Cr) and aminophenol (AP) and the inset of Fig. 6d demonstrates the CV performance for bare, rGO aerogel (rGOA), poly(aminopyrimidyl terthiophene) (pAPT), and *p*(APT–rGO) aerogel electrodes in 25 μM BPA solution. Among all four electrodes, the *p*(APT–rGO) aerogel showed the maximum current response, which is attributed to its extensive surface area, effective conductivity, and the interaction of charges with pAPT.[75] Zheng and Andou briefly reviewed on the detection and removal of the BPA endocrine disruptor using graphene-based materials.[10]

Gallic acid, a phenolic compound, is harmful for living bodies, therefore its detection and removal from wastewater is necessary. An N-doped graphene aerogel was utilized for the electrochemical detection of gallic acid. The oxidation of gallic acid at the N-doped graphene aerogel electrode can be confirmed by electrode performance before and after adding gallic acid to phosphate-buffered saline solution. Fig. 7a shows the absence of any oxidation peak in the cyclic voltammetry without adding gallic acid. Meanwhile, two oxidation peaks Q1 and Q2 were observed after the addition of gallic acid. The oxidation mechanism of gallic acid at the N-doped graphene aerogel electrode is displayed in Fig. 7b.
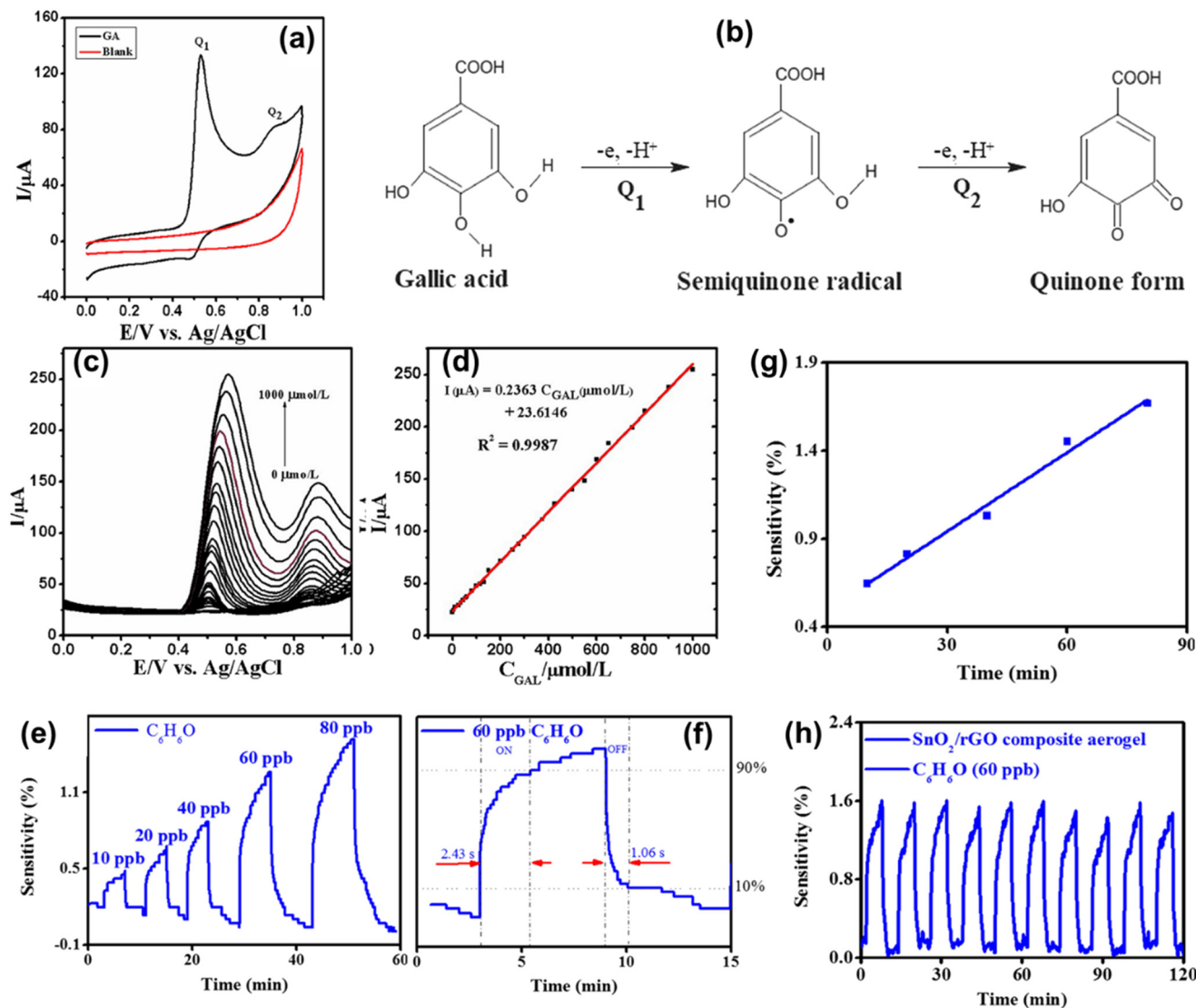
764 | *React. Chem. Eng.*, 2024, **9**, 753–776

This journal is © The Royal Society of Chemistry 2024

Fig. 7 (a) Schematic representation for synthesis of GAs–UiO-66-NH$_2$ and the sensing of heavy-metal ions; (b) differential pulse stripping voltammetry response of the GAs–UiO-66-NH$_2$ modified glassy carbon electrode after adding different concentrations of various metal ions to acetate buffer solution; reproduced from ref. 95 with permission from [American Chemical Society], copyright [2018]. (c) Fluorescence emission spectra of t-GA after addition of different toxic metals; (d) relative fluorescence intensity (I_0/I) of t-GA after addition of different metal ions; (e) the sensitivity of the rGO/SnO$_2$ based gas sensor to various phenol concentrations; (f) response and recovery times of the rGO/SnO$_2$ based gas sensor; (g) the sensitivity responses of the rGO/SnO$_2$ based gas sensor with various mass ratios to various phenol concentrations, and (h) the stability and repeatability test of the rGO/SnO$_2$ based gas sensor. Reproduced from ref. 92 with permission from [Elsevier Ltd], copyright [2015].

The differential pulse voltammetry technique was utilized for the detection of gallic acid in various concentrations at the N-doped graphene aerogel electrode with respect to Ag/AgCl in phosphate-buffered saline solution. Fig. 7c shows that even at a low concentration of gallic acid, an oxidation peak is observed and it increased with increasing concentration of gallic acid. These results indicated that the N-doped graphene aerogel is highly sensitive for gallic acid. In addition, the calibration curve shows a linear response of the peak current oxidation as a function of gallic acid concentration (Fig. 7d). rGO–metal-oxide aerogels were also explored for the detection of phenol with excellent stability, sensitivity and repeatability at room temperature as shown in

Fig. 7e–h. The electrical response of the prepared gas sensors increased with increasing concentration of phenol and followed a linear relationship as depicted in Fig. 7e and g, respectively. These sensors exhibited high sensitivity with a response time of 2.43 s and 1.06 s for recovery (Fig. 7f). A minimal reduction in the sensitivity was observed after undergoing ten detection cycles (Fig. 7h), which indicates significant repeatability of the gas sensors.[92] Stanley and colleagues developed a solvent assisted molybdenum nitride entrapped graphene aerogel heterostructure (MoN@GA) for the detection of the ronidazole drug. The electro-reduction of the ronidazole drug on the surface of the MoN@GA modified glassy carbon electrode involved the conversion of the nitro
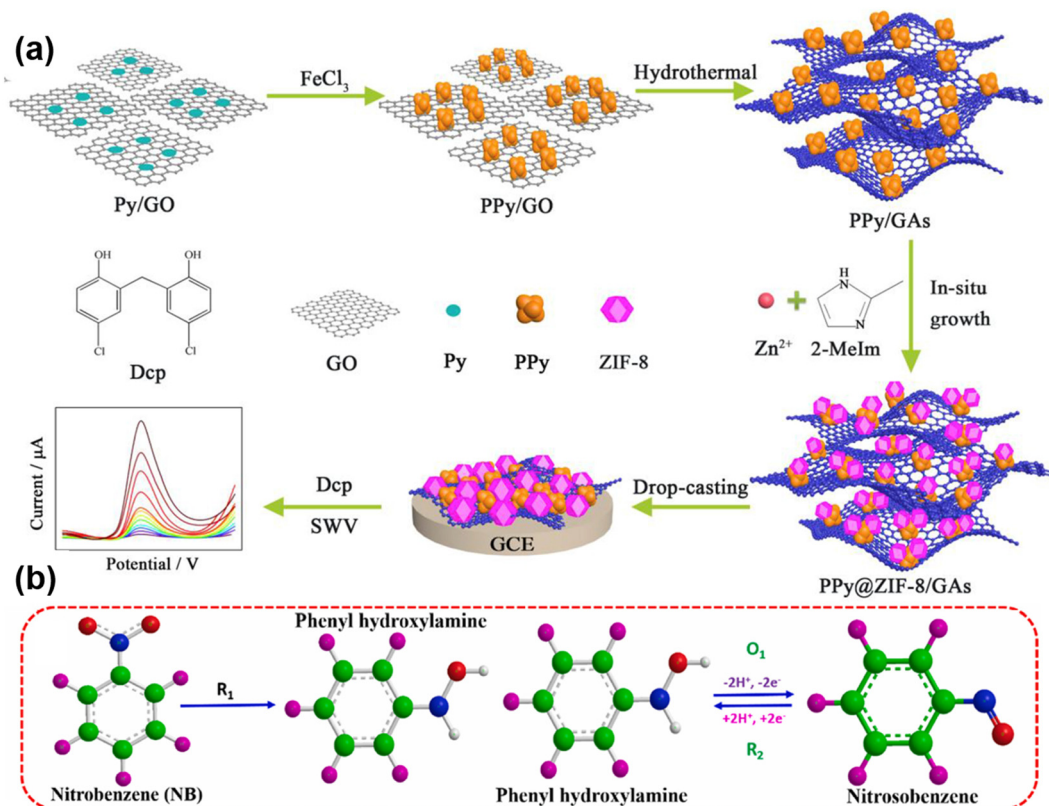
This journal is © The Royal Society of Chemistry 2024

React. Chem. Eng., 2024, **9**, 753–776 | **765**

Fig. 8 (a) Schematic representation for the synthesis of GAs/PPy@ZIF-8 and the sensing strategy for Dcp. Reproduced from ref. 96 with permission from [Elsevier Ltd], copyright [2019]. (b) The detection mechanism of nitrobenzene by SMO/N-rGO. Reproduced from ref. 97 with permission from [Elsevier Ltd], copyright [2023].

group of the ronidazole corresponding hydroxyl derivative through a four-proton, four-electron transfer mechanism.[93] Yan *et al.* engineered a honeycomb-like coarse pore, superelastic graphene aerogel structure suitable for strain or pressure sensing and particulate matter removal.[94] Based on the above discussion, it can be inferred that the functionalization might enhance the selectivity of graphene sensors. Functionalization of graphene incorporates additives with binding sites which can provide a major modification for graphene sensors through a lock-and-key binding mechanism. This strategy can provide selectivity for a wide range of chemical species as well as enable the identification of biological agents. Furthermore, the incorporation of foreign atoms like nitrogen, phosphorous, and boron into 3D graphene aerogels may provide a significant avenue for the fabrication of diverse sensors with favorable prospects in a wide range of applications.[13]

The composite porous polypyrrole@ZIF-8/graphene aerogels (PPy@ZIF-8/GAs) was utilized for the electrochemical detection of highly toxic 2,2-methylenebis (4-chlorophenol) (dichlorophenol, Dcp). The binding force between graphene aerogels and ZIF-8 effectively increased after the addition of PPy, which resulted in the excellent enhancement of electrochemical sensing of Dcp. The synthesis scheme of PPy@ZIF-8/GAs and the sensing strategy for Dcp are shown in Fig. 8a.[96] Karthik *et al.* decorated strontium molybdate

micro-flowers on a nitrogen rich graphene aerogel composite (SMO/N-rGO) using hydrothermal and precipitation techniques. The prepared sample was used for the detection of nitrobenzene from water. The detection mechanism of nitrobenzene by electrochemical reduction and redox reaction is summarized in Fig. 8b.[97] The increased content of N-doping in graphene aerogels was attributed to elevated electrical conductivity and greater specific surface area, resulting in heightened sensitivity to dopamine.[98] Metal–organic frameworks utilizing graphene aerogels showed excellent sensing ability towards emerging pollutants. For example, a metal–organic framework was used as an electrochemical sensor for the detection of catechol using copper centered GO aerogels. The prepared electrodes showed detection of catechol with a low detection limit and good repeatability, stability and reproducibility under the optimized conditions.[99]

Another class of emerging pollutants includes toxic NPs, which are widely used materials in a diverse range of applications such as biosensing,[100,101] energy storage devices,[102] energy conversion devices,[103] production of green hydrogen,[104] catalysts for organic transformation,[105] structural health monitoring,[106] orthodontics,[107] and biomedicine[108,109] depending on their properties. The increasing applications of NPs in every aspect of nanoscience and technology have given rise to a serious concern about their undesired presence in the environment. The toxicity

766 | *React. Chem. Eng.*, 2024, **9**, 753–776

This journal is © The Royal Society of Chemistry 2024

of nanomaterials may depend on their surface chemistry, mass number, size, surface area and composition.[110] These nanomaterials can enter the environment as primary particles or in complex matrices through disposal or industrial waste.[111] Carbon nanotubes have various applications in composite materials, electronic devices and energy storage.[112,113] However, certain types of carbon nanotubes cause respiratory issues when inhaled because of their potential toxicity.[114] Silver and gold NPs have antimicrobial properties and have been used in textiles, cosmetics, and household appliances. The release of silver and gold NPs into the environment concerns their effects on aquatic organisms and ecosystems.[115,116] A report by Kondratowicz *et al.* showed the removal of gold NPs *via* adsorption using graphene aerogels derived from GO.[116] The mass production and use of TiO_2 NPs in sunscreens, cosmetics, and food products because of their UV-absorbing and whitening properties make them easy to be released into aquatic environments, which further affects human health, aquatic animals, and even water ecosystems.[117] Toxicological studies show that ZnO NPs also harm humans and the environment. A research report shows that 3500 mg L^{-1} ZnO NPs were able to kill *Cyprinus carpio* at 50%- and 21 days of exposure. ZnO was found to affect the ovary, liver, and kidneys of *Cyprinus carpio*.[118]

ILs are a class of salts that exist in a liquid state at or below 100 °C. They have gained significant attention due to their unique properties, such as low volatility, high thermal stability, and good solubility for a wide range of compounds.[119] Although ILs have been widely explored for various industrial applications, they also raise concerns as potential emerging pollutants. ILs do not readily degrade, therefore they can accumulate in water bodies, sediments, and biota over time.[120] Some ILs show toxicity at higher concentration, which depends on their chemical structure as well as the nature of the cation and anion components.[121,122] ILs can enter the environment through improper disposal of IL containing products such as solvents, lubricants, and electrolytes used in various industrial applications. Furthermore, by organism uptake and subsequent bioaccumulation, ILs can enter the food chain. ILs consist of cations and anions; the generic structures of the compounds of organic cations and inorganic or organic anions are illustrated in Fig. 9.

The growth rate of algae *Scenedesmus quadricauda* and *Chlamydomonas reinhardtii* was found to gradually decrease in the presence of methylimidazolium (MIM) based ILs such as [1-butyl-3-MIM][Br], [1-hexyl-3-MIM][Br] and [1-octyl-3-MIM][Br].[123] Chu *et al.* demonstrated the toxicity mechanism of different ILs towards *Eisenia fetida* based on functional classification analysis. The toxic effect of ILs mainly arises from protein translation, modification and intracellular transport functions, which directly affect the catalytic activity and binding functions of proteins.[124] Protic ILs also show toxicity towards *Escherichia coli*, *Danio rerio* embryos and human skin cells.[125] Magina *et al.* reviewed the hazardous effect of ILs and discussed their biodegradability. Moreover, the ecological impact of ILs on various organisms and ecosystems along with fungi, bacteria and cell cultures was
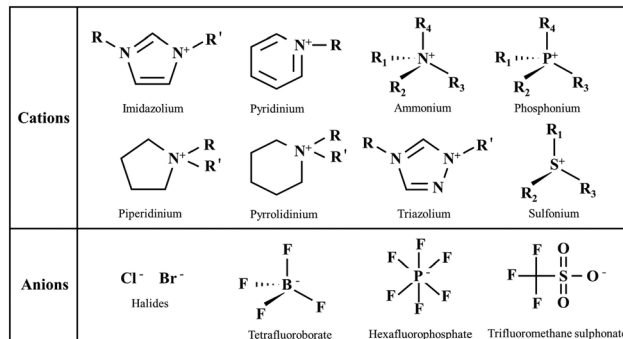

Fig. 9 Generic structures of common cations and anions of ILs. Reproduced from ref. 5 with permission from [Elsevier B.V.], copyright [2023].

also reviewed.[126] Although graphene aerogels are less explored in sensing of toxic nanomaterials and ILs, their morphological, mechanical and electrical properties position them as promising materials for the detection of these hazardous nanomaterials and ILs.

Overall, the utilization of graphene aerogels for the detection of emerging pollutants shows promise in providing rapid, sensitive, and selective analytical tools for environmental monitoring.[127]

4. Graphene aerogels for the remediation of emerging pollutants

Graphene aerogels have been demonstrated as promising materials for the remediation of emerging pollutants by different ways such as adsorption, photocatalysis, advanced oxidation and membrane filtration. In this section, we reviewed various processes for the remediation of emerging pollutants along with their proposed mechanism.

4.1 Graphene aerogel as an adsorbent

Adsorption is a traditional and promising approach in which emerging pollutants are attracted physically or chemically towards the surface of the adsorbent material, which leads to their removal from water.[128,129] Graphene-family nanomaterials such as 2D layers of carbon atoms, graphene, GO and rGO show excellent mechanical flexibility, high thermal stability and electrical conductivity.[9,130] Furthermore, their large specific surface area and the presence of abundant surface functional groups make them promising adsorbent materials for the remediation of emerging pollutants.[131] Graphene family nanosheets have a tendency to restack in water and it is very difficult to separate and reuse them.[12] To overcome these problems, 3D graphene aerogels are explored as an alternative to graphene assembled in 3D nanoarchitectures.[127]

The possible interaction in the adsorption process mainly involves π–π interaction, pore filling interaction, hydrophobic interaction, electrostatic attraction and repulsion, and hydrogen bonding.[23] The schematic representations for the removal of various emerging pollutants and the possible

This journal is © The Royal Society of Chemistry 2024

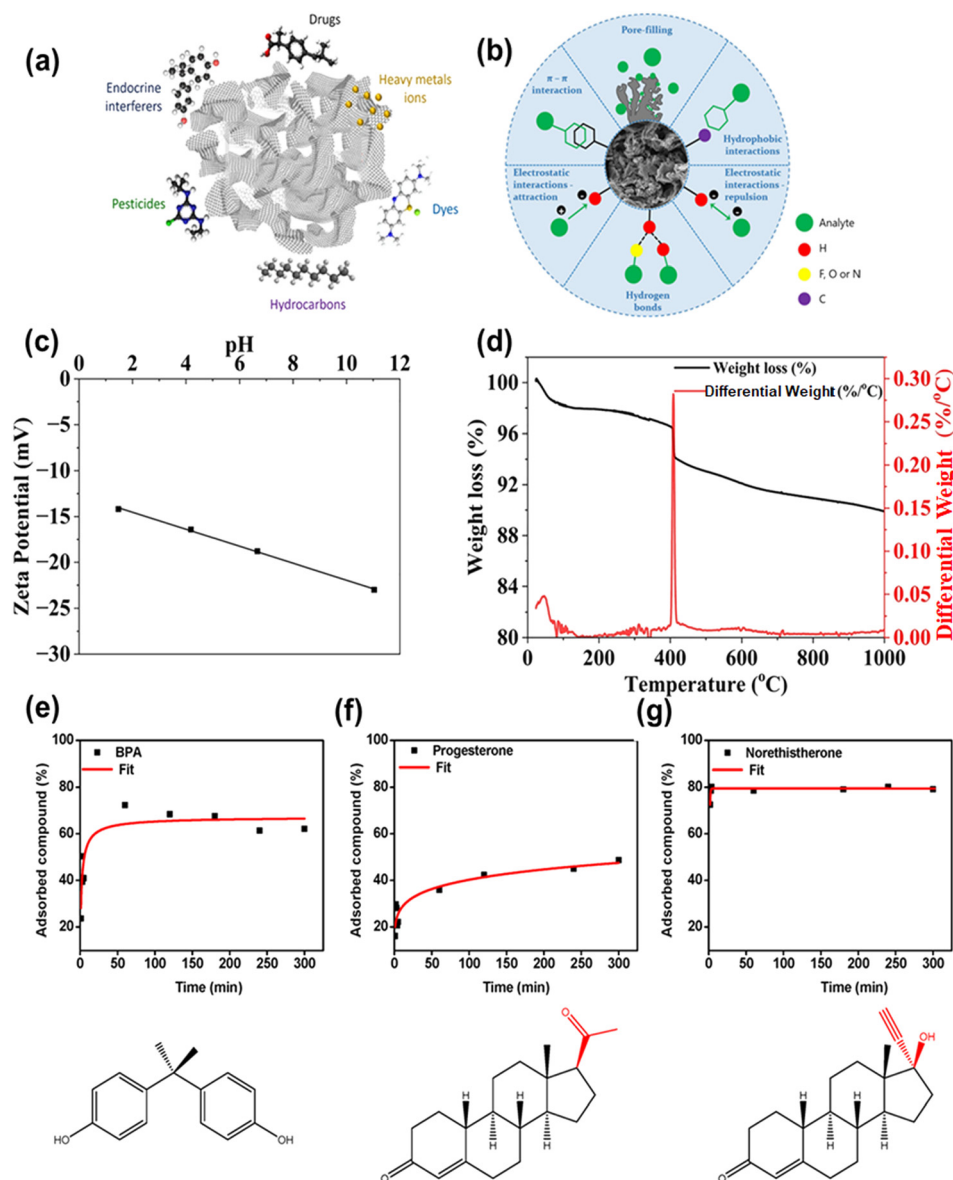*React. Chem. Eng.*, 2024, **9**, 753–776 | **767**

Fig. 10 (a) A schematic representation for the removal of various emerging pollutants by 3D graphene-based structures; (b) possible interaction mechanism for adsorption of emerging pollutants; reproduced from ref. 23 with permission from [Springer], copyright [2023]. (c) The zeta potential plot of the GO–SA at different pH values; (d) TGA plot of the mass loss of GO–SA. Reproduced from ref. 3 with permission from [*Scientific Reports*], copyright [2023]. Effect of incubation time on the removal percentage of (e) bisphenol A (BPA), (f) progesterone and (g) norethisterone. Reproduced from ref. 4 with permission from [Membranes], copyright [2020].

interaction with graphene aerogels are shown in Fig. 10a and b.[23] A GO doped silica aerogel (GO SA) was adopted for the removal of harmful dyes and emerging pollutants from wastewater. Fig. 10c shows the negative zeta potential of the GO SA at different pH values, which was due to the presence of partially negatively charged silanol groups (–Si–OH) on its surface.[3] The adsorption of sulfamethoxazole (SMA) onto the GO SA occurred *via* weak intermolecular forces. These forces do not depend on pH. The adsorption sequence starts with particles swiftly moving from the solution to the adsorbent, succeeded by gradual diffusion of particles hindered by mass transfer resistance. As repulsion forces between pollutants in the adsorbent and the liquid

phase intensify, particle diffusion decelerates. Ultimately, active sites become saturated, and the process concludes.[3] The thermal stability of the GO SA was analyzed by TGA (Fig. 10d), and only 2% weight loss at high temperature was observed. The calcination of coating occurred after the weight loss, which makes the material hydrophobic, and as a result the adsorption capacity decreased.[3] Furthermore, magnetic GO based foam (graphene oxide–polyethyleneimine–iron nanoparticle composite (GO–PEI–FeNPs)) was utilized for the adsorption of emerging pollutants such as BPA, progesterone and norethisterone swiftly moving from the solution to the adsorbent. Fig. 10(e–g) presents the percentage adsorption of endocrine disruptors as a function of time. The maximum

768 | *React. Chem. Eng.*, 2024, **9**, 753–776

This journal is © The Royal Society of Chemistry 2024

adsorbed BPA compound was 68% after 60 min (Fig. 10e). The adsorbed progesterone was 48% after 5 h (Fig. 10f) and norethisterone adsorption was 80% after 30 min. (Fig. 10g).[4] The different adsorption behaviors of the various endocrine disruptors may be attributed to the different adsorption mechanisms. Specifically, all three studied compounds have C sp^2 bonding which allows robust π–π interaction with the GO plane. In addition, the adsorption may take place *via* hydrogen bonding between the GO foam and hydroxyl groups in BPA, and the ketone and alkyne groups in norethisterone. In the case of progesterone, having only two ketone groups, interactions with the foam may be less potent with respect to its interactions with BPA and norethisterone, potentially elucidating the membrane's lower adsorption of progesterone.[4] Fang *et al.* demonstrated a magnesium ascorbyl phosphate derived non-shell graphene-based monolith (MAP-GBM) for the adsorption of BPA. The shift in the O–H stretching band after BPA adsorption in the FTIR spectrum confirmed the hydrogen bonding between unreacted oxygen-containing groups MAP-GBM and hydroxyl groups of BPAs. After adsorption of BPA, the shift in skeletal C=C vibrations identified the π–π interaction between MAP-GBM and BPA. Electrostatic interaction and a hydrophobic effect were also observed at pH less than 7.[56] In addition, the adsorption mechanism of ciprofloxacin on the surface of a graphene–boron nitride composite aerogel illustrated that the exceptional adsorption performance of the composite foam was primarily attributed to the synergistic interactions between boron nitride, graphene nanoplatelets, and the functional groups of ciprofloxacin.[58]

Doping of foreign atoms enhances the adsorption capacity of graphene aerogels towards emerging pollutants. In this regard, Liu *et al.* reported the doping of fluorine and the loading of copper in a graphene aerogel (Cu/F-rGA) to enhance the adsorption of aqueous perfluorooctanoic acid. The results showed that after fluorine doping and copper NP loading, the adsorption capacity of perfluorooctanoic acid on Cu/F-rGA increased. The hydrogen bonding, hydrophobic interaction, F–F interaction and ligand exchange reaction played a significant role in the adsorption mechanism.[57] The surface functionalization of graphene aerogels may enhance the adsorption of emerging pollutants from wastewater. An amidoxime-functionalized carboxymethyl β-cyclodextrin based graphene aerogel *via* a hydrothermal process was utilized for the selective adsorption of uranium. The maximum adsorption capacity was found to be 654.2 mg g^{-1} as calculated using the Langmuir model.[132] The hydrothermal assisted graphene aerogel was functionalized using fluoroalkylsilane by a vapor–liquid deposition technique. The prepared superhydrophobic and superoleophilic graphene aerogel showed enormous adsorption capacities for the selective removal of organic pollutants from an oil–water mixture.[133] Liu *et al.* and Bordin *et al.* recently reviewed graphene aerogel-based materials for the effective adsorption of pollutants from wastewater.[23,134] However, some challenges such as developing environmentally friendly large-scale production, optimizing adsorption capacity

and understanding the potential impact of graphene particles on the environment need to be addressed when using graphene aerogels as adsorbents for the remediation of emerging pollutants. In this process, the pollutants adsorbed on the surface and within the pores of the graphene aerogel, yet they persist in the environment.

4.2 Graphene aerogel as a photocatalyst

Photocatalysis is a process in which a material absorbs photons and uses the optical energy to promote chemical reactions without being consumed. Photocatalytic degradation is an effective, low cost, excellent oxidation ability and ecofriendly technology which make it superior over other competing processes for the complete degradation of emerging pollutants from wastewater. Various materials such as ZnO,[135] TiO$_2$,[136] BiVO$_4$,[137] Bi$_2$S$_3$,[137] WS$_2$,[55] *etc.* have been utilized as photocatalysts. However, their low visible-light absorption efficiency, the high recombination rate of charge carriers, and the complicated removal of the catalyst from the treated water limit their industrial applications.[138] Graphene aerogels have highly accessible active sites, a tunable band gap, high stability and reusability, and high hydrophobicity, which make them promising materials as photocatalysts for the remediation of emerging pollutants.

To enhance the photocatalytic degradation activity of graphene aerogels, a few layers of WS$_2$ nanosheets were *in situ* grown into the nanopores of an N-doped graphene aerogel (WNGA) for the degradation of caffeine under visible light. The proposed pathways of photodegradation of caffeine are illustrated in Fig. 11a.[55] When the visible light is incident on the surface of the WNGA photocatalyst, induced ˙OH reacts with the imidazole ring of caffeine to produce *m/z* 210 (C1), *m/z* 229 (C2), and *m/z* 246 (C3) as shown in pathway I (Fig. 11a). Alternatively, *m/z* 181 (C4), *m/z* 166 (C5) and *m/z* 166 (C6) can be produced by attacks of ˙OH and ˙O$_2^-$ on N-demethylation of caffeine as represented in pathway II (Fig. 11a). These intermediate products may perform ring fragmentation reactions in the presence of reactive oxygen species and holes which result in formation of various low-molecular-weight hydrocarbons (C7–C12) which are finally mineralized to NO$_3^-$, H$_2$O, CO$_2$, and NH$_4^+$.[55] For incessant and efficient degradation of emerging pollutants from water, microspheres of silver phosphate and GO aerogel (SGAM) with radially oriented microchannels were developed.[139] The efficient photodegradation activity was due to the incorporation of silver phosphate in the honeycomb structure of the GO aerogel because of the interaction between silver phosphate and GO sheets, which accelerates the electron transfer (Fig. 11b). The proposed degradation of BPA under visible light in the presence of SGAM is illustrated in Fig. 11c.[139] The photodegradation mechanism for degradation of organic pollutants using graphitic carbon nitride (g-C$_3$N$_4$)–ZnO@graphene aerogel (g-C$_3$N$_4$–ZnO@GA) heterojunctions is demonstrated in Fig. 11d.[135] The Z scheme e$^-$ transfer mode can be seen in these heterojunction

This journal is © The Royal Society of Chemistry 2024

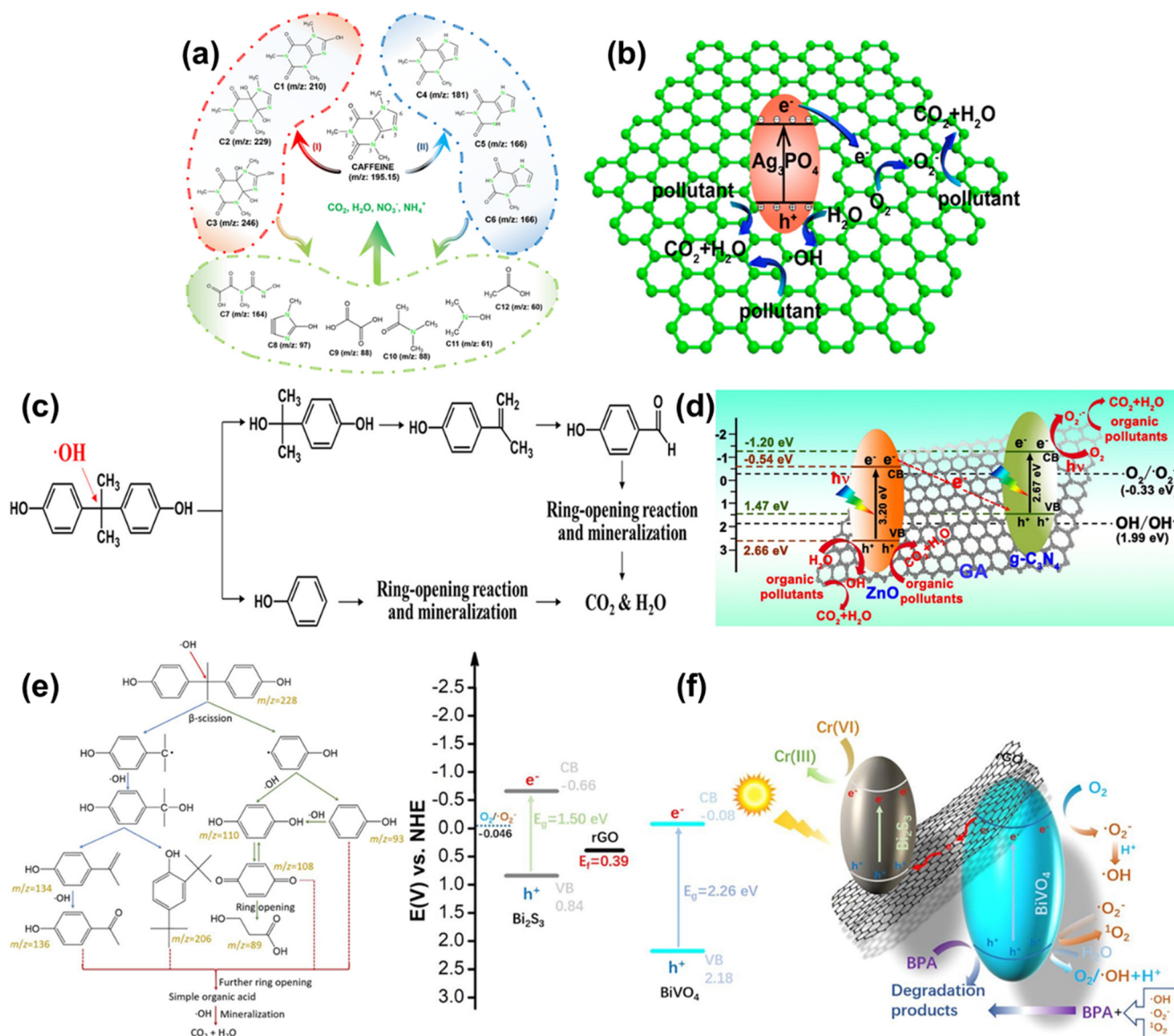*React. Chem. Eng.*, 2024, **9**, 753–776 | **769**

Fig. 11 (a) Plausible pathways for the photocatalytic degradation of caffeine over WNGA under visible-light irradiation; reproduced from ref. 55 with permission from [American Chemical Society], copyright 2024. (b) Schematic illustration of the charge transfer and the pollutant degradation on SGAM. (c) Proposed photocatalytic degradation pathway of BPA in the presence of SGAM. Reproduced from ref. 139 with permission from [American Chemical Society], copyright [2019]. (d) Photocatalytic representation of the g-C$_3$N$_4$–ZnO@GA heterojunction; reproduced from ref. 135 with permission from [Elsevier B.V.], copyright [2019]. (e) Proposed photocatalytic degradation pathway of BPA. (f) Schematic of the possible band diagram and charge transfer scheme of SVGA; reproduced from ref. 137 with permission from [Elsevier B.V.], copyright [2019].

structures. When UV light is irradiated on the surface of g-C$_3$N$_4$–ZnO@GA, e$^-$ becomes excited from the VB to the CB of both ZnO and g-C$_3$N$_4$, generating e$^-$ and h$^+$. e$^-$ in the CB of ZnO quickly recombines with the h$^+$ in the VB of g-C$_3$N$_4$ through the conductive layer of the graphene aerogel. As a result, e$^-$ and h$^+$ are left in the VB of ZnO and the CB of g-C$_3$N$_4$, respectively. The e$^-$ in the CB of g-C$_3$N$_4$ reacts with O$_2$ and the h$^+$ in the VB of ZnO reacts with –OH from H$_2$O to form strong oxidizing agents $^\cdot$O$_2^-$ and $^\cdot$OH radicals, respectively.[135] Based on the Z-scheme, Liang *et al.* proposed the photodegradation of BPA by a heterojunction system using a bismuth sulphide (Bi$_2$S$_3$) and bismuth vanadate (BiVO$_4$) based graphene aerogel (SVGA). The proposed

pathway for the degradation of BPA in the presence of g-C$_3$N$_4$–ZnO@GA is shown in Fig. 11e.[137] The proposed mechanism shows that the photoinduced e$^-$ in the CB of BiVO$_4$ recombines with the h$^+$ in the VB of Bi$_2$S$_3$ through the conducting reduced graphene oxide of the graphene aerogel (Fig. 11f).[137] This results in efficient accumulation of e$^-$ in the CB of Bi$_2$S$_3$, enhancing the reduction ability of Bi$_2$S$_3$. Meanwhile, the accumulation of h$^+$ will take place in the VB of BiVO$_4$, leading to production of radicals, and these h$^+$ and radicals contribute to degradation of BPA.[137] Nawaz *et al.* utilized a hydrothermal process for the synthesis of a porous 3D rGO/TiO$_2$ aerogel (RGOT) for the photodegradation of carbamazepine in aqueous medium. The prepared 3D
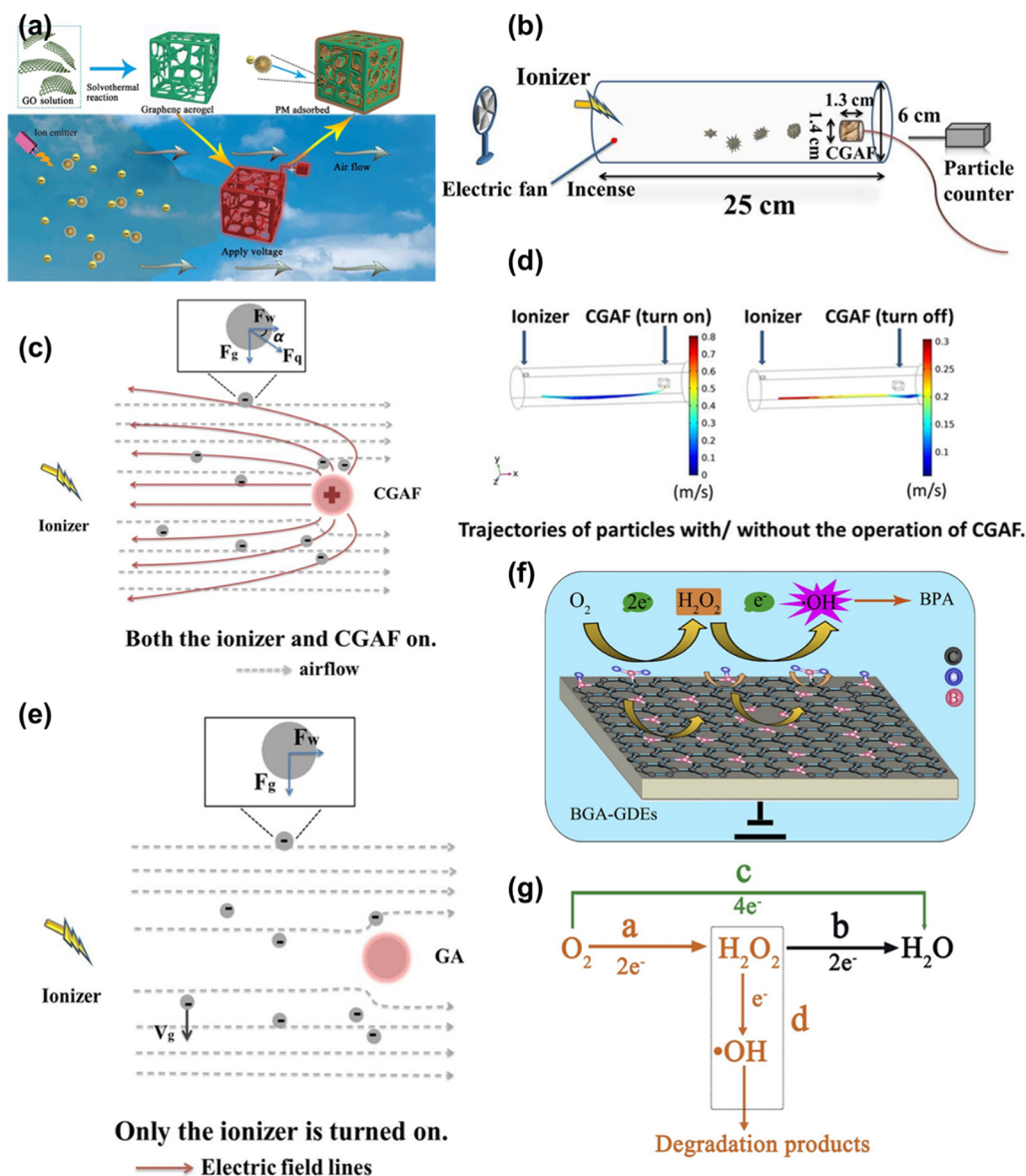
Fig. 12 (a) Schematic illustration of the CGAF used to remove PM; (b) the schematic of the device used for the removal of PM; (c) when the CGAF is off, the PM mainly experiences two main forces; (d) when the ionizer is turned on in the presence of the CGAF; (e) COMSOL simulation of the trajectory of PM in different situations (the CGAF is on and off); reproduced from ref. 141 with permission from [Elsevier B.V.], copyright [2020]. (f) Schematic illustration of *in situ* metal-free EAOPs with BGA-GDEs; (g) schematic illustration of possible mechanisms of EAOPs. Reproduced from ref. 142 with permission from [Elsevier B.V.], copyright [2019].

macroporous structure showed effective charge separation and mass transport of carbamazepine near the TiO_2 surface, making it a promising photocatalyst. The rGO played an important role in the accumulation of e^- transported from the CB of TiO_2.[136] Zhang *et al.* synthesized a Bi_2O_3 supported carbon fiber aerogel for continuous and stable removal of antibiotics without any separation operation.[14] Fang *et al.* developed TiO_2 nanotube pillared graphene-based macrostructures for continuous removal of emerging pollutants from water. The prepared sample removed almost 86% of BPA at an initial concentration of 0.05 mg L^{-1} under Xe lamp irradiation in a continuous flow system.[56] Another study by Jiang *et al.* revealed the efficient removal of BPA

using a boron/N-doped graphene aerogel *via* photocatalysis under visible light.[140] Hasanpour *et al.* reviewed the photocatalytic activity of aerogels for removal of various pollutants from wastewater.[138] However, there are some challenges that need to be addressed while using graphene aerogels for the remediation of emerging pollutants including developing optimization of photocatalytic efficiency and enhancing selectivity for specific contaminants.

4.3 Other techniques

In addition to the above discussed methods, there are some other techniques and mechanisms by which graphene

This journal is © The Royal Society of Chemistry 2024

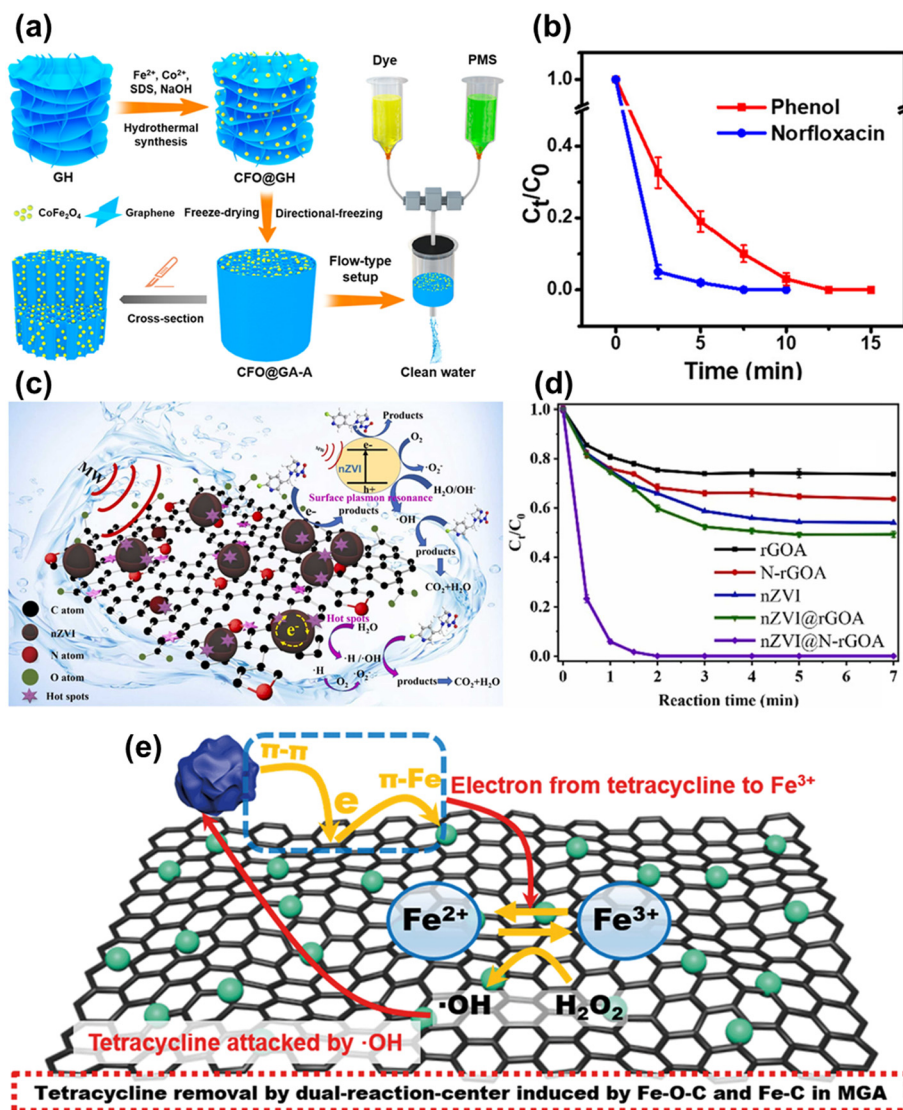*React. Chem. Eng.*, 2024, **9**, 753–776 | 771

Fig. 13 (a) A schematic illustration of the preparation of an anisotropic $CoFe_2O_4$@graphene hybrid aerogel and its application for continuous treatment of wastewater with a flow-type setup. (b) Plots of the relative concentration change of norfloxacin and phenol with time. Reproduced from ref. 144 with permission from [American Chemical Society], copyright [2019]. (c) Proposed mechanism for imidacloprid removal by an nZVI supported N-rGO aerogel. (d) Imidacloprid removal profiles of different catalysts at room temperature by microwave irradiation. Reproduced from ref. 64 with permission from [Elsevier B.V.], copyright [2023]. (e) Mechanism for removal of antibiotics by MGA. Reproduced from ref. 145 with permission from [The Royal Society of Chemistry], copyright [2019].

aerogels are utilized for water reclamation. These methods leverage the excellent properties of graphene aerogels for the remediation of different types of emerging pollutants from wastewater. Zhao *et al.* prepared an active, reusable, and flame-retardant charged graphene aerogel filter (CGAF) for the removal of particulate matter (PM) under external electric force as shown in Fig. 12a.[141] As displayed in Fig. 12b, a fan and stick are used at one end of a pipe to simulate the ongoing release of vehicle exhaust. An ionizer is incorporated into the device to enable the negative charge on PM. The negatively charged PM is attracted towards the positively charged CGAF.[141] Fig. 12c illustrates three types of forces, gravity, wind force and electrostatic force, on PM when the ionizer is turned on in the presence of an electric field on the CGAF. Meanwhile, wind force and gravitational force are

exerted on PM in the absence of an electric field on the CGAF when the ionizer is on as demonstrated in Fig. 12e.[141] The removal efficiency of the CGAF without an electric field was found to be almost 50% because in this case, sedimentation coupled with aggregation takes place among the PM solely through electrostatic interaction. Fig. 12d shows the COMSOL simulation results for the trajectory of PM in both cases which are consistent with the actual situation.[141] A metal-free electrocatalysis technique was adopted for the removal of BPA using a boron-doped graphene aerogel modified gas diffusion electrode (BGA-GDE). The proposed mechanism for the removal of BPA is demonstrated in Fig. 12f.[142] A principal pathway exists for the electrochemical reactions between electrons and migrated O_2 on the electrode. In this process, two electron reduction of O_2

772 | *React. Chem. Eng.*, 2024, **9**, 753–776

This journal is © The Royal Society of Chemistry 2024

generates H_2O_2, which subsequently transforms *via in situ* activation into ˙OH radicals using the same electrons. Knowingly, the introduction of diverse "activation sites" occurs due to the formation environments of various B-doped states within graphene nanosheets. Within BGA-GDEs, three distinct types of bonds –BCO_2, –BC_2O and –BC_3 are present, and the excellent electrocatalytic performance can be potentially attributed to the synergistic interplay of these different B-bond configurations.[142] Fig. 12g presents the possible mechanism of the electrochemical advanced oxidation process. The initial reaction source O_2 can undergo two pathways.[142] Similarly, an N-doped graphene aerogel was used as a particle electrode for electrocatalytic advanced oxidation of simulated BPA.[143] Wang *et al.* synthesized an N-doped 3D graphene aerogel by a hydrothermal method. The prepared sample showed exceptional catalytic activities in peroxymonosulfate activation and was utilized for the removal of ibuprofen from water by oxidative degradation.[63]

Graphene aerogel-based polymer composites are also widely used for the remediation of emerging pollutants through rapid catalytic degradation. A $CoFe_2O_4$ incorporated graphene hybrid aerogel was developed for the catalytic degradation of phenol and norfloxacin. Fig. 13a presents the schematic illustration of the synthesis and water treatment application of the hybrid aerogel in a flow type setup.[144] Fig. 13b demonstrates that norfloxacin and phenol were completely removed in 7.5 and 12.5 min, respectively.[144] Microwave assisted degradation was also utilized for the removal of emerging water contaminants. An N-doped rGO aerogel showed superefficient degradation of imidacloprid in polluted water.[64] The proposed reaction mechanism for the removal of imidacloprid by an nZVI supported N-rGO aerogel in the presence of microwave irradiation is depicted in Fig. 13c.[64] Additionally, the nZVI supported N-rGO aerogel showed higher microwave degradation of imidacloprid as compared to the rGO aerogel, N-rGO aerogel, nZVI, and nZVI supported rGO aerogel (Fig. 13d).[64] Zhuang *et al.* proposed polymer template assisted synthesis of an Fe_3O_4@Fe/graphene aerogel (MGA) for the removal of antibiotics. Fig. 13e presents the possible mechanism for the pollutant removal using MGA.[145] Tetracycline strongly adsorbs on the surface of graphene *via* robust π–π interactions and hydrogen bonding, and works as an electron donor. Subsequently, the electrons within the tetracycline may transfer towards iron species *via* graphene through π–Fe interactions. This mechanism would speed up the conversion of Fe(II) from Fe(III). As a result, π–π interactions combined with π–Fe interactions promoted the removal efficiency with the acceleration of adsorption and degradation.[145]

5. Conclusion and future perspectives

Through an extensive review of literature, it is evident that graphene aerogels have been a trending material due to their unique and exceptional properties such as high surface area, tailored porosity, and outstanding adsorption capacities.

Sustainable biomass derived graphene aerogels address environmental concerns as well as align with the principles of green chemistry, which leads to the development of economically viable and environmentally friendly solutions for water remediation. The effective removal of a diverse array of emerging pollutants such as pharmaceuticals, toxic NPs, dyes, and ionic liquids highlights the potential flexibility and practicality of biomass-based graphene aerogels in water remediation.

However, it is indispensable to acknowledge the existing challenges, such as large-scale production, ensuring cost-effectiveness, and developing well-organized reproduction methods for graphene aerogels. Optimizing synthesis parameters, such as precursor composition, temperature, and activation conditions for various biomass materials to enhance the performance and reproducibility of graphene aerogels that can meet the demands of industrial applications is a future concern. Surface functionalization and pore structure tailoring of different biomass-based graphene aerogels to introduce specific functional groups for the enhancement of adsorption sites and better selectivity towards emerging pollutants are still challenging. Additionally, the long-term stability and durability and adsorption efficiency of specific pollutants are the ongoing challenges. The toxicity and biological safety of biomass-derived graphene aerogels are crucial considerations, especially when these materials may come into contact with living organisms. It's important to note that the biological safety of graphene aerogels highly depends on graphene derivatives, the amount of materials and the synthesis method. *In vivo* studies using animal models are crucial for assessing the biological safety of graphene aerogels. In addition, studies on the biodistribution, metabolism, and potential long-term effects are necessary. However, natural source-derived graphene aerogels, owing to their natural origin, are often considered to be more biocompatible.

Looking ahead, future research should prioritize the engineering of synthesis procedures to realize optimal material features, tailor-made for specific pollutant classes. Additionally, investigation of hybrid systems with improved pollutant removal abilities by the synergistic combinations of graphene aerogels with other advanced materials needs to be explored. Development of graphene aerogel-based membranes for efficient water filtration. Long-term performance and industrial application studies are important to authenticate the long-term efficacy and viability of biomass-derived graphene aerogels in practical wastewater treatment scenarios. Furthermore, the incorporation of data-driven approaches and analytical modeling could facilitate the strategy and optimization of these materials for targeted pollutant removal.

In essence, biomass-based graphene aerogels display significant potential as a sustainable and effective solution for reducing the impact of emerging pollutants in wastewater. Continued interdisciplinary research and a holistic approach to addressing challenges will pave the way for the successful deployment of these innovative materials,

This journal is © The Royal Society of Chemistry 2024

React. Chem. Eng., 2024, **9**, 753–776 | **773**

contributing to the preservation of water quality and the overall well-being of our ecosystems.

Conflicts of interest

There are no conflicts to declare.

Acknowledgements

References

1 M. Arumugam, K.-K. Seralathan, S. Praserthdam, M. Tahir and P. Praserthdam, *Chemosphere*, 2022, **303**, 135121.

2 P. P. Das, A. D. Sontakke, N. S. Samanta and M. K. Purkait, in *Industrial Wastewater Reuse: Applications, Prospects and Challenges*, Springer, 2023, pp. 63–87.

3 S. K. Sharma, P. Ranjani, H. Mamane and R. Kumar, *Sci. Rep.*, 2023, **13**, 16448.

4 J. N'Diaye, S. Poorahong, O. Hmam, G. C. Jiménez, R. Izquierdo and M. Siaj, *Membranes*, 2020, **10**, 340.

5 H. Ren, H. Qian, Q. Hou, W. Li and M. Ju, *Sep. Purif. Technol.*, 2023, **310**, 123112.

6 P. Kumari, K. M. Tripathi, L. K. Jangir, R. Gupta and K. Awasthi, *Mater. Today Chem.*, 2021, **22**, 100597.

7 S. K. Fanourakis, J. Peña-Bahamonde, P. C. Bandara and D. F. Rodrigues, *npj Clean Water*, 2020, **3**, 1.

8 T. Russo, P. Fucile, R. Giacometti and F. Sannino, *Processes*, 2021, **9**, 719.

9 C. Lee, X. Wei, J. W. Kysar and J. Hone, *Science*, 2008, **321**, 385–388.

10 A. Zheng and Y. Andou, *Int. J. Environ. Sci. Technol.*, 2022, **19**, 6869–6888.

11 Z. Bano, S. A. Mazari, R. Y. Saeed, M. A. Majeed, M. Xia, A. Q. Memon, R. Abro and F. Wang, *J. Water Process Eng.*, 2020, **36**, 101404.

12 F. Liu and T. S. Seo, *Adv. Funct. Mater.*, 2010, **20**, 1930–1936.

13 Y. Shen, Q. Fang and B. Chen, *Environ. Sci. Technol.*, 2015, **49**, 67–84.

14 P. Zhang, L. Yin, X. Yang, J. Wang, M. Chi and J. Qiu, *Carbon*, 2023, **201**, 110–119.

15 H. Xie, Z. He, Y. Liu, C. Zhao, B. Guo, C. Zhu and J. Xu, *ACS Omega*, 2022, **7**, 7638–7647.

16 T. S. C. Almeida da Silva, L. Marchiori, B. Oliveira Mattos, S. Ullah, H. D. S. Barud, R. Romano Domeneguetti, H. D. Rojas-Mantilla, M. V. Boldrin Zanoni, U. P. Rodrigues-Filho and E. P. Ferreira-Neto, *ACS Appl. Mater. Interfaces*, 2023, **15**, 23146–23159.

17 A. Ehsani, M. Esfahaniha, P. Khodaei kahriz, R. Safari and H. Parsimehr, *Surf. Interfaces*, 2021, **22**, 100817.

18 M.-Y. Kim, H. Park, J.-Y. Lee, D. J. Park, J.-Y. Lee, N. V. Myung and K. H. Lee, *J. Chem. Eng.*, 2022, **431**, 134250.

19 L. Lin, Q. Xie, M. Zhang, C. Liu, Y. Zhang, G. Wang, P. Zou, J. Zeng, H. Chen and M. Zhao, *Colloids Surf., A*, 2020, **601**, 124978.

20 J. Kaushik, V. Kumar, A. K. Garg, P. Dubey, K. M. Tripathi and S. K. Sonkar, *New J. Chem.*, 2021, **45**, 9073–9083.

21 X. Zhuang, J. Liu, Q. Zhang, C. Wang, H. Zhan and L. Ma, *Renewable Sustainable Energy Rev.*, 2022, **154**, 111877.

22 Y. Wang, M. Zhang, X. Shen, H. Wang, H. Wang, K. Xia, Z. Yin and Y. Zhang, *Small*, 2021, **17**, 2008079.

23 M. B. Leão, J. R. Bordin and C. F. de Matos, *Water, Air, Soil Pollut.*, 2023, **234**, 136.

24 H. Ren, X. Shi, J. Zhu, Y. Zhang, Y. Bi and L. Zhang, *J. Mater. Sci.*, 2016, **51**, 6419–6427.

25 Y.-Q. Li, Y. A. Samad, K. Polychronopoulou, S. M. Alhassan and K. Liao, *ACS Sustainable Chem. Eng.*, 2014, **2**, 1492–1497.

26 Y. Bin, Q. Liang, H. Luo, Y. Chen and T. Wang, *Environ. Sci. Pollut. Res.*, 2023, **30**, 6746–6757.

27 I. Lee, S.-M. Kang, S.-C. Jang, G.-W. Lee, H. E. Shim, M. Rethinasabapathy, C. Roh and Y. S. Huh, *J. Mater. Chem. A*, 2019, **7**, 1737–1748.

28 F. Wu, D. Liu, G. Li, L. Li, L. Yan, G. Hong and X. Zhang, *Nanoscale*, 2021, **13**, 5419–5428.

29 N. Li, L. Yang, D. Wang, C. Tang, W. Deng and Z. Wang, *Environ. Sci. Technol.*, 2021, **55**, 9181–9188.

30 K. Pang, X. Song, Z. Xu, X. Liu, Y. Liu, L. Zhong, Y. Peng, J. Wang, J. Zhou and F. Meng, *Sci. Adv.*, 2020, **6**, eabd4045.

31 S. Shukla, I. Khan, V. K. Bajpai, H. Lee, T. Kim, A. Upadhyay, Y. S. Huh, Y.-K. Han and K. M. Tripathi, *ACS Appl. Mater. Interfaces*, 2019, **11**, 18165–18177.

32 S. Wei, X. Qiu, J. An, Z. Chen and X. Zhang, *Compos. Sci. Technol.*, 2021, **207**, 108730.

33 X. Huang, G. Yu, Y. Zhang, M. Zhang and G. Shao, *J. Chem. Eng.*, 2021, **426**, 131894.

34 L. Cao, C. Wang and Y. Huang, *J. Chem. Eng.*, 2023, **454**, 140094.

35 J. Zhang, S. Luo, Y. Ma, R. Li, Y. Jin, L. Qiu and W. Zhang, *Chin. Chem. Lett.*, 2023, **34**, 107363.

36 S. P. Lee, G. A. Ali, M. A. Assiri, K. V. Kong, E. Y. L. Teo and K. F. Chong, *Appl. Surf. Sci.*, 2023, **613**, 156069.

37 D. K. Singh, V. Kumar, S. Mohan and S. H. Hasan, *J. Chem. Eng. Data*, 2017, **62**, 1732–1742.

38 Z.-S. Wu, S. Yang, Y. Sun, K. Parvez, X. Feng and K. Müllen, *J. Am. Chem. Soc.*, 2012, **134**, 9082–9085.

39 T. Ma, Y. Kong, H. Liu, X. Xu, Q. Yue, B. Gao and Y. Gao, *J. Colloid Interface Sci.*, 2023, **633**, 628–639.

40 Z. Song, W. Liu, N. Sun, W. Wei, Z. Zhang, H. Liu, G. Liu and Z. Zhao, *Solid State Commun.*, 2019, **287**, 27–30.

41 Y. Myung, S. Jung, T. T. Tung, K. M. Tripathi and T. Kim, *ACS Sustainable Chem. Eng.*, 2019, **7**, 3772–3782.

42 V. K. Bajpai, S. Shukla, I. Khan, S.-M. Kang, Y. Haldorai, K. M. Tripathi, S. Jung, L. Chen, T. Kim and Y. S. Huh, *ACS Appl. Mater. Interfaces*, 2019, **11**, 43949–43963.

43 R. Shadkam, M. Naderi, A. Ghazitabar, A. Asghari-Alamdari and S. Shateri, *Ceram. Int.*, 2020, **46**, 22197–22207.

44 X. Zhang, Z. Sui, B. Xu, S. Yue, Y. Luo, W. Zhan and B. Liu, *J. Mater. Chem. A*, 2011, **21**, 6494–6497.

774 | *React. Chem. Eng.*, 2024, **9**, 753–776

This journal is © The Royal Society of Chemistry 2024

45 S. Bi, L. Zhang, C. Mu, M. Liu and X. Hu, *Appl. Surf. Sci.*, 2017, **412**, 529–536.

46 T. T. P. N. X. Trinh, T. H. Quan, T. N. M. Anh, D. B. Thinh, N. T. Lan, D. N. Trinh, N. M. Dat, H. M. Nam, M. T. Phong and N. H. Hieu, *Surf. Interfaces*, 2021, **23**, 101023.

47 L. Xu, G. Xiao, C. Chen, R. Li, Y. Mai, G. Sun and D. Yan, *J. Mater. Chem. A*, 2015, **3**, 7498–7504.

48 J. Liang, Z. Cai, L. Li, L. Guo and J. Geng, *RSC Adv.*, 2014, **4**, 4843–4847.

49 A. Wang, S. Bok, R. Thiruvengadathan, K. Gangopadhyay, J. A. McFarland, M. R. Maschmann and S. Gangopadhyay, *Combust. Flame*, 2018, **196**, 400–406.

50 H. Zhang, X. Liu, B. Wang, Z. Shi, Z. Wei, Z. Wu, Y. Zhu, Q. Guo and X. Wang, *J. Chem. Eng.*, 2023, **465**, 142943.

51 Z. Chen, W. Ren, L. Gao, B. Liu, S. Pei and H.-M. Cheng, *Nat. Mater.*, 2011, **10**, 424–428.

52 S. Long, H. Wang, K. He, C. Zhou, G. Zeng, Y. Lu, M. Cheng, B. Song, Y. Yang and Z. Wang, *Colloids Surf., A*, 2020, **594**, 124666.

53 Q. Li, Z. Sun, C. Yin, Y. Chen, D. Pan, B. Yu, Y. Zhang, T. He and S. Chen, *J. Chem. Eng.*, 2023, 141492.

54 Y. Ma, M. Yu, J. Liu, X. Li and S. Li, *ACS Appl. Mater. Interfaces*, 2017, **9**, 27127–27134.

55 T. Shafi, C. Das, B. K. Dubey and S. Chowdhury, *ACS Appl. Nano Mater.*, 2024, **7**, 1723–1737.

56 Z. Fang, Y. Hu, J. Cheng and Y. Chen, *J. Chem. Eng.*, 2019, **372**, 581–589.

57 L. Liu, N. Che, S. Wang, Y. Liu and C. Li, *ACS Omega*, 2021, **6**, 7073–7085.

58 L. Han, A. M. E. Khalil, J. Wang, Y. Chen, F. Li, H. Chang, H. Zhang, X. Liu, G. Li, Q. Jia and S. Zhang, *Sep. Purif. Technol.*, 2021, **278**, 119605.

59 D. B. Thinh, T. H. Tu, N. M. Dat, T. T. Hong, P. T. N. Cam, D. N. Trinh, H. M. Nam, M. T. Phong and N. H. Hieu, *Surf. Interfaces*, 2021, **26**, 101309.

60 P. Joshi, O. P. Sharma, S. K. Ganguly, M. Srivastava and O. P. Khatri, *J. Colloid Interface Sci.*, 2022, **608**, 2870–2883.

61 C. Chen, F. Li, Y. Zhang, B. Wang, Y. Fan, X. Wang and R. Sun, *J. Chem. Eng.*, 2018, **350**, 173–180.

62 J. Kaushik, V. Kumar, K. M. Tripathi and S. K. Sonkar, *Chemosphere*, 2022, **287**, 132225.

63 J. Wang, X. Duan, Q. Dong, F. Meng, X. Tan, S. Liu and S. Wang, *Carbon*, 2019, **144**, 781–790.

64 P. Zhang, X. Meng, M. Fan, S. Wu, C. Wang, X. Shang, H. Jia and H. Sun, *Appl. Catal., B*, 2024, **340**, 123258.

65 S. Elhenawy, M. Khraisheh, F. AlMomani, M. K. Hassan, M. A. Al-Ghouti and R. Selvaraj, *Nanomaterials*, 2021, **12**, 87.

66 M. Liu, X. Liu, P. Wang and X. Zhang, *Colloids Surf., A*, 2021, **626**, 126886.

67 T. Letcher and D. A. Vallero, *Waste: A handbook for management*, Academic Press, 2019.

68 P. Kumari, K. M. Tripathi, K. Awasthi and R. Gupta, *Ind. Eng. Chem. Res.*, 2023, **62**, 13837–13847.

69 P. G. S. A. JeyaSundar, A. Ali and Z. Zhang, in *Microorganisms for sustainable environment and health*, Elsevier, 2020, pp. 119–135.

70 I. B. Chabchoubi, S. S. Lam, S. E. Pane, M. Ksibi, G. Guerriero and O. Hentati, *Environ. Pollut.*, 2022, 120698.

71 C. D. Iwu, L. Korsten and A. I. Okoh, *Microbiology*, 2020, **9**, e1035.

72 J. Xiao, Y. Tan, Y. Song and Q. Zheng, *J. Mater. Chem. A*, 2018, **6**, 9074–9080.

73 L. Liu, G. Kong, Y. Zhu, D. Lai, S. Zhang and C. Che, *Appl. Surf. Sci.*, 2022, **598**, 153694.

74 H. Mater Mahnashi, A. M. Mahmoud, A. Saad Alkahtani and M. M. El-Wekil, *Microchem. J.*, 2021, **163**, 105925.

75 M.-Y. Kim, K.-D. Seo, H. Park, R. G. Mahmudunnabi, K. Hwan Lee and Y.-B. Shim, *Appl. Surf. Sci.*, 2022, **604**, 154430.

76 L. Interdonato, R. Siracusa, R. Fusco, S. Cuzzocrea and R. Di Paola, *Int. J. Mol. Sci.*, 2023, **24**, 5682.

77 S. A. Berghuis, A. F. Bos, P. J. Sauer and E. Roze, *Arch. Toxicol.*, 2015, **89**, 687–709.

78 S.-M. Ho, A. Cheong, M. A. Adgent, J. Veevers, A. A. Suen, N. N. Tam, Y.-K. Leung, W. N. Jefferson and C. J. Williams, *Reprod. Toxicol.*, 2017, **68**, 85–104.

79 D. Cuomo, I. Porreca, G. Cobellis, R. Tarallo, G. Nassa, G. Falco, A. Nardone, F. Rizzo, M. Mallardo, C. J. M. Ambrosino and C. Endocrinology, *Mol. Cell. Endocrinol.*, 2017, **457**, 20–34.

80 I. Gültekin and N. H. Ince, *J. Environ. Manage.*, 2007, **85**, 816–832.

81 R. Jasrotia and S. Tabassum, *Impact of Endocrine Toxicants on a Sustainable Environment*, Apple Academic Press, 2023.

82 E. Asenuga and A. Olagunju, *African Journal of Health, Safety and Environment*, 2023, **4**, 57–66.

83 J. Płotka-Wasylka, E. Mulkiewicz, H. Lis, K. Godlewska, A. Kurowska-Susdorf, M. Sajid, D. Lambropoulou and N. Jatkowska, *Sci. Total Environ.*, 2023, **881**, 163350.

84 A. Rathipriya, D. Agarwal, E. Suresh and M. A. Rather, in *Xenobiotics in Aquatic Animals: Reproductive and Developmental Impacts*, Springer, 2023, pp. 415–427.

85 L. N. Vandenberg, R. Hauser, M. Marcus, N. Olea and W. V. Welshons, *Reprod. Toxicol.*, 2007, **24**, 139–177.

86 A. Colin, C. Bach, C. Rosin, J.-F. Munoz and X. Dauchy, *Arch. Environ. Contam. Toxicol.*, 2014, **66**, 86–99.

87 T. Yamamoto, A. Yasuhara, H. Shiraishi and O. Nakasugi, *Chemosphere*, 2001, **42**, 415–418.

88 T. T. Tuyet-Hanh, L. Vu-Anh, N. Ngoc-Bich and T. Tenkate, *Int. J. Environ. Res. Public Health*, 2010, **7**, 2395–2406.

89 H. Ishiniwa, M. Sakai, S. Tohma, H. Matsuki, Y. Takahashi, H. Kajiwara and T. Sekijima, *Ecotoxicology*, 2013, **22**, 1335–1347.

90 J. R. Pilsner, M. Parker, O. Sergeyev and A. Suvorov, *Reprod. Toxicol.*, 2017, **69**, 221–229.

91 M. K. Manibusan and L. W. Touart, *Crit. Rev. Toxicol.*, 2017, **47**, 440–488.

92 D. Guo, P. Cai, J. Sun, W. He, X. Wu, T. Zhang, X. Wang and X. Zhang, *Carbon*, 2016, **99**, 571–578.

93 M. M. Stanley, S.-F. Wang, J. N. Baby, B. Sriram and M. George, *J. Mol. Liq.*, 2023, **375**, 121308.

94 S. Yan, G. Zhang, F. Li, L. Zhang, S. Wang, H. Zhao, Q. Ge and H. Li, *Nanoscale*, 2019, **11**, 10372–10380.

95 M. Lu, Y. Deng, Y. Luo, J. Lv, T. Li, J. Xu, S.-W. Chen and J. Wang, *Anal. Chem.*, 2018, **91**, 888–895.

96 Y. Xie, X. Tu, X. Ma, M. Xiao, G. Liu, F. Qu, R. Dai, L. Lu and W. Wang, *Electrochim. Acta*, 2019, **311**, 114–122.

97 R. Karthik, P. R. Chavan, R. Sukanya, G. Dhakal, J.-J. Shim and C. B. Breslin, *Composites, Part B*, 2023, **256**, 110649.

98 S. Ai, Y. Chen, Y. Liu, Q. Zhang, L. Xiong, H. Huang, L. Li, X. Yu and L. Wei, *Solid State Sci.*, 2018, **86**, 6–11.

99 Y. Xu, Y. Yu, S. Xue, X. Ma and H. Tao, *J. Electroanal. Chem.*, 2021, **899**, 115686.

100 I. Kucherenko, O. Soldatkin, D. Y. Kucherenko, O. Soldatkina and S. Dzyadevych, *Nanoscale Adv.*, 2019, **1**, 4560–4577.

101 K. S. Raju, G. S. Das and K. M. Tripathi, *RSC Sustainability*, 2024, **2**, 223–232.

102 G. S. Das, R. Panigrahi, S. Ghosh and K. M. Tripathi, *Mater. Today Sustain.*, 2024, **25**, 100656.

103 H.-P. Feng, L. Tang, G.-M. Zeng, Y. Zhou, Y.-C. Deng, X. Ren, B. Song, C. Liang, M.-Y. Wei and J.-F. Yu, *Adv. Colloid Interface Sci.*, 2019, **267**, 26–46.

104 R. Aggarwal, S. K. Sonkar and K. M. Tripathi, *Carbon*, 2023, **208**, 436–442.

105 J. Kaushik, C. Sharma, N. K. Lamba, P. Sharma, G. S. Das, K. M. Tripathi, R. K. Joshi and S. K. Sonkar, *Langmuir*, 2023, **39**, 12865–12877.

106 G. S. Das, V. K. Tripathi, J. Dwivedi, L. K. Jangir and K. M. Tripathi, *Nanoscale*, 2023, **16**, 1490.

107 W. Zakrzewski, M. Dobrzynski, W. Dobrzynski, A. Zawadzka-Knefel, M. Janecki, K. Kurek, A. Lubojanski, M. Szymonowicz, Z. Rybak and R. J. Wiglusz, *Nanomaterials*, 2021, **11**, 337.

108 Y. Zhao, Z. Zhang, Z. Pan and Y. Liu, *Exploration*, 2021, **1**, 20210089.

109 M. Park, A. Sharma, C. Kang, J. Han, K. M. Tripathi and H.-J. Lee, *ACS Biomater. Sci. Eng.*, 2022, **8**, 2131–2141.

110 T. A. Saleh, *Environ. Technol. Innovation*, 2020, **20**, 101067.

111 Z. Zahra, Z. Habib, S. Hyun and M. Sajid, *Sustainability*, 2022, **14**, 2041.

112 G. S. Das, S. Sarkar, R. Aggarwal, S. K. Sonkar, J.-W. Park, K. M. Tripathi and T. Kim, *Carbon Lett.*, 2019, **29**, 595–603.

113 S. K. Sonkar, K. M. Tripathi and S. Sarkar, *J. Nanosci. Nanotechnol.*, 2014, **14**, 2532–2538.

114 S. K. Prajapati, A. Malaiya, P. Kesharwani, D. Soni and A. Jain, *Drug Chem. Toxicol.*, 2022, **45**, 435–450.

115 G. R. Tortella, O. Rubilar, N. Durán, M. C. Diez, M. Martínez, J. Parada and A. B. Seabra, *J. Hazard. Mater.*, 2020, **390**, 121974.

116 I. Kondratowicz, K. Żelechowska, M. Nadolska, A. Jażdżewska and M. Gazda, *Colloids Surf., A*, 2017, **528**, 65–73.

117 Y. Kuang, H. Guo, K. Ouyang, X. Wang, D. Li and L. Li, *Comp. Biochem. Physiol., Part C: Toxicol. Pharmacol.*, 2023, **266**, 109548.

118 A. G. Hashim and Y. F. K. Al Fatlawy, *Journal of Wasit for Science and Medicine*, 2023, **16**, 26–39.

119 G. Kaur, H. Kumar and M. Singla, *J. Mol. Liq.*, 2022, **351**, 118556.

120 A. Oskarsson and M. C. Wright, *Environ. Sci. Technol.*, 2019, **53**, 10539–10541.

121 M. Sivapragasam, M. Moniruzzaman and M. Goto, *Biotechnol. J.*, 2020, **15**, 1900073.

122 C.-W. Cho, T. P. T. Pham, Y. Zhao, S. Stolte and Y.-S. Yun, *Sci. Total Environ.*, 2021, **786**, 147309.

123 K. J. Kulacki and G. A. Lamberti, *Green Chem.*, 2008, **10**, 104–110.

124 L. Chu, X. Hou, X. Song, X. Zhao, S. Hu and G. Shen, *Sci. Total Environ.*, 2023, **875**, 162411.

125 M. R. Ortega Vega, E. K. Baldin, D. P. Pereira, M. C. S. Martins, P. Pranke, F. Horn, I. Pinheiro, A. Vieira, B. Espiña, S. Mattedi and C. D. F. Malfatti, *J. Hazard. Mater.*, 2022, **422**, 126896.

126 S. Magina, A. Barros-Timmons, S. P. Ventura and D. V. Evtuguin, *J. Hazard. Mater.*, 2021, **412**, 125215.

127 A. K. Kasar, S. Tian, G. Xiong and P. L. Menezes, *J. Porous Mater.*, 2022, **29**, 1011–1025.

128 P. Kumari, K. M. Tripathi, K. Awasthi and R. Gupta, *Environ. Sci. Pollut. Res.*, 2023, **30**, 15480–15489.

129 B. Bhaduri, A. K. Dikshit, T. Kim and K. M. Tripathi, *ACS Appl. Nano Mater.*, 2022, **5**, 16000–16026.

130 A. K. Geim and K. S. Novoselov, *Nat. Mater.*, 2007, **6**, 183–191.

131 X. Wu, J. Zhou, W. Xing, G. Wang, H. Cui, S. Zhuo, Q. Xue, Z. Yan and S. Z. Qiao, *J. Mater. Chem. A*, 2012, **22**, 23186–23193.

132 N. Li, L. Yang, D. Wang, C. Tang, W. Deng and Z. Wang, *Environ. Sci. Technol.*, 2021, **55**, 9181–9188.

133 H. Wang, C. Wang, S. Liu, L. Chen and S. Yang, *RSC Adv.*, 2019, **9**, 8569–8574.

134 Y.-P. Liu, Y.-T. Lv, J.-F. Guan, F. M. Khoso, X.-Y. Jiang, J. Chen, W.-J. Li and J.-G. Yu, *J. Mol. Liq.*, 2021, **343**, 117709.

135 J.-Y. Zhang, J.-Y. Mei, S.-S. Yi and X.-X. Guan, *Appl. Surf. Sci.*, 2019, **492**, 808–817.

136 M. Nawaz, W. Miran, J. Jang and D. S. Lee, *Appl. Catal., B*, 2017, **203**, 85–95.

137 Q. Liang, S. Ploychompoo, J. Chen, T. Zhou and H. Luo, *J. Chem. Eng.*, 2020, **384**, 123256.

138 M. Hasanpour and M. Hatami, *J. Mol. Liq.*, 2020, **309**, 113094.

139 Y. Liu, D. Yang, Y. Shi, L. Song, R. Yu, J. Qu and Z.-Z. Yu, *ACS Sustainable Chem. Eng.*, 2019, **7**, 11228–11240.

140 Y. Jiang, S. Chowdhury and R. Balasubramanian, *J. Environ. Chem. Eng.*, 2020, **8**, 104300.

141 K. Zhao, J. Huang, J. Mao, Z. Bao, Z. Chen and Y. Lai, *J. Chem. Eng.*, 2020, **395**, 125086.

142 P. Wu, Y. Zhang, Z. Chen, Y. Duan, Y. Lai, Q. Fang, F. Wang and S. Li, *Appl. Catal., B*, 2019, **255**, 117784.

143 Z. Chen, Y. Zhang, L. Zhou, H. Zhu, F. Wan, Y. Wang and D. Zhang, *J. Hazard. Mater.*, 2017, **332**, 70–78.

144 X.-J. Yu, J. Qu, Z. Yuan, P. Min, S.-M. Hao, Z.-S. Zhu, X. Li, D. Yang and Z.-Z. Yu, *ACS Appl. Mater. Interfaces*, 2019, **11**, 34222–34231.

145 Y. Zhuang, X. Wang, L. Zhang, D. D. Dionysiou and B. Shi, *Environ. Sci.: Nano*, 2019, **6**, 3232–3241.